University of New Hampshire
University of New Hampshire Scholars' Repository

Master's Theses and Capstones | Student Scholarship

Spring 2017

Effects of small-scale turbulence on phytoplankton growth and metabolism

Wilton Gray Burns
University of New Hampshire, Durham

Follow this and additional works at: https://scholars.unh.edu/thesis

Recommended Citation

Burns, Wilton Gray, "Effects of small-scale turbulence on phytoplankton growth and metabolism" (2017). *Master's Theses and Capstones*. 1113.
https://scholars.unh.edu/thesis/1113

This Thesis is brought to you for free and open access by the Student Scholarship at University of New Hampshire Scholars' Repository. It has been accepted for inclusion in Master's Theses and Capstones by an authorized administrator of University of New Hampshire Scholars' Repository. For more information, please contact Scholarly.Communication@unh.edu.

EFFECTS OF SMALL-SCALE TURBULENCE ON PHYTOPLANKTON GROWTH AND METABOLISM

By

WILTON GRAY BURNS

BS Environmental Science, University of North Carolina – Chapel Hill, 2014

THESIS

Submitted to the University of New Hampshire

in Partial Fulfillment of

the Requirements for the Degree of

Master of Science

in

Oceanography

May, 2017

This thesis has been examined and approved in partial fulfillment of the requirements for the degree of Master of Science in Oceanography by:

Thesis Director, Dr. Kai Ziervogel, Research Assistant Professor of Biogeochemistry/Microbial Ecology

Dr. Tim Moore, Research Assistant Professor of Bio-Optics and Remote Sensing

Dr. Adrian Marchetti, Assistant Professor in Marine Science
University of North Carolina – Chapel Hill

On April 3, 2017

Original approval signatures are on file with the University of New Hampshire Graduate School

Acknowledgements

First, thank you Mom for encouraging me to pursue a career in science and thanks Dad for being proud beyond belief and always asking questions about my project. Also, thank you Jordan for showing up in my life at a very opportune time - your support and friendship have made this degree possible.

Thank you to the mentors who have inspired me, encouraged me to pursue a graduate degree in Oceanography, and given counsel throughout my Master's thesis work – Natalie Cohen, Kelsey Ellis, Mike Sieracki, Nicole Poulton, Peter Countway, and Kimberly DeLong,

Thank you to my committee members Kai Ziervogel, Tim Moore, and Adrian Marchetti for your guidance and help in preparing this thesis. I greatly appreciated the insights shared on experimental design set-up, data collection, and interpretation of this dataset.

Kai, I am so thankful for your mentorship these past few years. You showed me how much fun a career in academia can (and should) be through your passion for marine science and amazing perspective on life that inspired me every day. I know I will continue to be a happy and successful scientist if I keep some of your words of wisdom in mind throughout my career.

Finally, I would like to thank the University of New Hampshire for the resources invested in me. This degree was funded by the UNH Department of Earth Sciences Teaching Assistantships, a NH Sea Grant Research Assistantship, the UNH Graduate School Summer TA Fellowship Award, the William R. Spaulding Marine Program Endowment, the ESCI Student Research Fund, and the UNH Oceanography Program. This work is part of a larger NSF-funded project (NSF OCE-1335088). Additionally, thanks to the School of Marine Sciences and Ocean Engineering for bringing together the marine scientists at UNH and fostering a close-knit scientific community.

Table of Contents

Abstract

EFFECTS OF SMALL SCALE TURBULENCE ON PHYTOPLANKTON GROWTH AND METABOLISM

By

Wilton Gray Burns

University of New Hampshire, May, 2017

Our current understanding of how turbulence affects small planktonic organisms is based on fluid dynamic theory, ocean models, and laboratory experiments that often have conflicting results. Atmospheric models predict that global temperature rise associated with climate change will affect turbulence patterns within the marine photic zone, where phytoplankton reside. To investigate how small-scale turbulence affects growth (growth rates, cell counts and extracted chlorophyll, and nutrient quotas) and metabolism (production of transparent exopolymer particles (TEP)) of marine primary producers, phytoplankton in monoculture and natural assemblages were incubated under a range of turbulent treatments. Results indicate that early in exponential growth of the monocultures, cell-specific TEP was higher with increased turbulence. During mid- and late exponential growth, there were no measurable differences in phytoplankton growth and TEP production as a function of turbulence. However, nutrient quotas were higher in the more turbulent tanks with phytoplankton cells >15 μm in length. Data from this study suggest that changes in turbulence in marine photic zones could result in increased nutrient storage in larger phytoplankton cells, as predicted by numerical models, but may not greatly affect the global carbon cycle via changes in TEP production.

1. Introduction

Phytoplankton form the base of the marine food web and play an integral role in the sequestration of atmospheric carbon to the deep ocean through a mechanism known as the biological pump (DeVries et al., 2012). Marine microorganisms have long been studied by biological oceanographers for the role they play in the global carbon and oxygen cycles. With impending global climate change affecting chemical and physical ocean properties, there exists an even more compelling argument to study marine microbes because there could be shifts in their ecological functions (Edwards and Richardson, 2004; Montes-Hugo et al., 2009; Toseland et al., 2013). For instance, data from community-derived coupled atmosphere-wave models suggest atmospheric temperature rise could result in robust changes in ocean surface winds, wave heights, and wave periods in the late 21st century (Fan et al., 2013; Hemer et al., 2013a).

Air temperature and surface winds interact with the surface of the ocean and create mixing in the upper portion of the water column, directly influencing physical parameters in marine photic zones via turbulence, meaning secondary motion caused by moving fluids. Changes in turbulence in the surface ocean would affect environmental conditions for phytoplankton that reside in marine surface waters (Fan et al., 2013; Hemer et al., 2013a, 2013b). Some models predict a ~25% decrease and ~7% increase in annual mean significant wave height in the global ocean area due to the effects of global climate change (Hemer et al., 2013a) (Figure 1). Decreases in wave heights will likely occur in every ocean except the Southern Ocean, where increased wave heights and periods are expected (Fan et al., 2013; Hemer et al., 2013a, 2013b) (Figure 1). Waves propagate northward from Southern Ocean and increased wave heights and periods in that region may have a substantial effect on global ocean wave patterns (Hemer et al., 2013a). Future changes in wave could lead to changes in water mixing in the surface ocean,

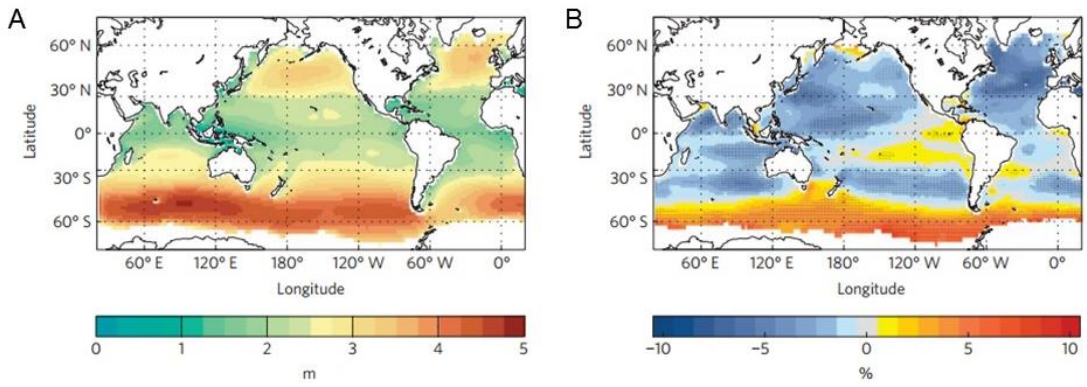

Figure 1 | Present (A, 1979 – 2009) significant annual wave heights (m) and projected changes (B, 2070 - 2100) in annual wave heights (% change) averaged from multiple models. Figure adapted from Hemer et al. 2013.

affecting turbulence in marine photic zones (Fan et al., 2013; Hemer et al., 2013a, 2013a). Additionally, field observations have demonstrated that the interaction of air temperature and surface wind forcings can induce mixing, enhancing nutrient supply to the photic zone via upwelling from the deep ocean associated with a deepening mixed layer (Fan et al., 2013; Rumyantseva et al., 2015). Primary productivity is stimulated during and after periods of high wind forcing because nutrients from the deep ocean are brought up to the surface via water mixing (Rumyantseva et al., 2015). A major factor in determining phytoplankton trophic state and community structure is nutrient availability (Hecky and Kilham, 1988). Nutrients are the limiting factor for phytoplankton growth in areas of downwelling and water column stratification because surface waters do not have many nutrient inputs.

Larger scale mixing will also affect turbulence on the scale of individual planktonic cells (i.e. small-scale turbulence), which is a major driver for nutrient fluxes from the surrounding water to the cell (Barton et al., 2014; Karp-Boss et al., 1996). Numerical models demonstrate that there is a region of lower nutrient concentration around planktonic cells that can be perturbed by small-scale turbulence and positively impact nutrient assimilation in phytoplankton cells (Barton

et al., 2014; Karp-Boss et al., 1996; Wolf-Gladrow and Riebesell, 1997). The physical environment around individual phytoplankton cells can change with increased turbulence when the rate of nutrient absorption across the cell membrane is happening faster than the rate of diffusion of nutrients towards the cell (Barton et al., 2014; Karp-Boss et al., 1996). This difference in rates creates an area around the cell, the nutrient concentration boundary layer, where nutrients are lower than in the surrounding water (Jumars, 1993; Karp-Boss et al., 1996; Koch, 1971). Nutrient concentration boundary layers do not have definitive boundaries but can be defined as when concentration of nutrients surrounding the cell is <90% that of the ambient water (Karp-Boss et al., 1996). Disruption can occur when the diameter of the nutrient concentration boundary layer approaches the length of the smallest turbulent eddies, called Kolmogorov length scales (Karp-Boss et al., 1996; Kolmogorov, 1962). Disruption decreases the distance that nutrients from the ambient water have to diffuse towards the cell, potentially increasing the amount of nutrients that reach cell membranes (Karp-Boss et al., 1996). Under normal oceanic conditions, fluid dynamic theory predicts that only cells >60 µm in diameter approach Kolmogorov length scales in open ocean ecosystems and experience a disruption of the nutrient concentration boundary layer (Karp-Boss et al., 1996). The handful of laboratory experiments show inconsistencies with fluid dynamic theory and suggest that small-scale turbulence in the surface ocean affects planktonic organisms in a way that is still under debate (Arin et al., 2002; Hondzo and Lyn, 1999; Hondzo and Wüest, 2009; Iversen et al., 2010; Peters et al., 2006; Thomas and Gibson, 1990). A few mesocosms have found that community composition and size were affected by turbulence and that growth of large cells was favored in the higher turbulent treatments (Arin et al., 2002; Iversen et al., 2010). Conversely, several laboratory studies found that growth of two nanoplankton was actually inhibited with increasing

small-scale turbulence (Hondzo and Lyn, 1999; Peters et al., 2006; Thomas and Gibson, 1990). The phytoplankton cells used in this study are technically below the Kolmogorov length scale for the range of turbulent environments tested, so the individual cells should not "feel" the effects of turbulence. However, monocultures and experiments with natural assemblages found a positive relationship between small-scale turbulence and growth of heterotrophic bacteria, nanoplankton, and microplankton even when the cells were well below the Kolmogorov length scales (Beauvais et al., 2006; Hondzo and Wüest, 2009; Iversen et al., 2010; Mari and Robert, 2008; Thomas and Gibson, 1990).

Despite the fact that small-scale turbulence might significantly increase the flux of nutrients towards large phytoplankton cells, most models do not include how phytoplankton metabolic processes might be affected by this change in nutrients (Barton et al., 2014; Ross, 2006; Ruiz, 1996). Phytoplankton cells become stressed, meaning they cannot reach their maximum potential growth rate, when nutrient concentrations are below a certain threshold (Brand et al., 1981). An increased nutrient flux in high turbulent conditions could have implications on the stress levels and metabolic processes in phytoplankton cells.

One of the important metabolic processes that could be affected by turbulence is the role phytoplankton play by contributing to the dissolved organic matter (DOM) pool. Throughout their normal cellular processes, phytoplankton and bacteria release DOM into the water column. A large portion of this plankton-derived DOM pool forms the basis for transparent exopolymer particles (TEP) (Passow, 2002b). TEP is a highly surface-reactive (sticky) biofilm that serves as the underlying matrix for sinking marine aggregates (Alldredge and Silver, 1988; Engel, 2000; Grossart et al., 2006; Kiørboe et al., 1990, 1994; Mari et al., 2005; Riebesell et al., 1995). The importance of TEP with respect to carbon export was demonstrated by Martin et al. (2011) who

found high levels of TEP associated with phytoplankton aggregates in sediment trap samples shortly after a diatom spring bloom in the sub-polar North Atlantic Ocean. One method of predicting the export of carbon in the ocean is combining ocean color satellite observations and measurements of organic carbon levels in the surface ocean with microbial food web models (Siegel et al., 2014). Another, more direct, measurement of organic carbon flux from the photic to aphotic zone is provided by sediment trap deployments that collect sinking marine snow at specific water depths over a certain period of time (Riebesell et al., 1995). These current methods for estimating global carbon export in the ocean leave open questions about biogeochemical processes that help understand the fate of atmospherically fixed organic carbon during its sinking through the water column. Insights into the smaller scale processes can be obtained from laboratory experiments and later combined with the current methods to obtain more accurate estimates for carbon export in the ocean. Understanding the relationship between changes in turbulence and TEP production will be paramount in predicting the effects of global climate change on the biological pump (Armstrong et al., 2001).

Some of the mesocosm experiments that found higher growth with increasing turbulent conditions also found increased volumetric TEP in high turbulent conditions (Beauvais et al., 2006; Iversen et al., 2010). These studies did not investigate whether the positive relationship between TEP and turbulence was due to the higher phytoplankton growth, so this study further examines phytoplankton metabolism and the relationship between turbulence and production of DOM. Other potential ecological stressors that could impact phytoplankton growth and metabolism (ie. light intensity) are minimized in this study and to investigate how changes in small-scale turbulence affect nutrient dynamics in phytoplankton cells. Generally, when phytoplankton cells are stressed, TEP production increases (Mari et al., 2005; Passow and Laws,

2015). One proposed mechanism for the positive relationship between stress and TEP production is that by releasing their excess organic matter to the surrounding water, cells can increase their ability to respond metabolically to other environmental conditions i.e. decoupling growth rate from photosynthesis if that suddenly became energetically favorable (Passow and Laws, 2015). In these incubations if the cells in the high turbulent treatments experience an increased flux of nutrients, it is possible that TEP production will decrease because an increase nutrient flux would minimize any nutrient stress that could be happening with the phytoplankton cells. Additionally, TEP production will likely be lower in the higher turbulent treatments because if the cells are growing at a faster rate (due to an increased nutrient flux), the organic carbon fixed through photosynthesis will likely be put towards cell growth and division rather than be released as DOM into the water column.

The overarching goal of this study is to better understand the role turbulence plays in nutrient fluxes, and how TEP production is impacted. This study uses oscillating grids, one of the most commonly used apparatuses to study the effects of small-scale turbulence on plankton dynamics, to subject multiple phytoplankton types to a range of homogenous turbulence levels (Alldredge et al., 1990; Guadayol et al., 2009; Hondzo and Lyn, 1999; Hondzo and Wüest, 2009; Peters et al., 2006).

2. Hypotheses

i. For both the monocultures and natural assemblages, turbulence will cause an increased flux of nutrients towards phytoplankton cell membranes, regardless of cell size, resulting in higher growth rates and nutrient quotas in the high mixing treatments.

ii. For both the monocultures and natural assemblages, this increased flux of nutrients will lead to lower cell/chlorophyll-specific TEP in the higher mixing tanks because the cells will be less stressed and producing less TEP per cell/unit chlorophyll, than in the lower turbulent conditions.

3. Materials and Methods

3.1 Oscillating grid set-up

Experiments with monocultures and natural assemblages were conducted in cylindrical acrylic tanks (height: 195 mm; diameter: 140 mm). Homogenous small-scale turbulence in the tanks was generated by circular grids (diameter: 125 mm) that oscillate at specific frequencies in

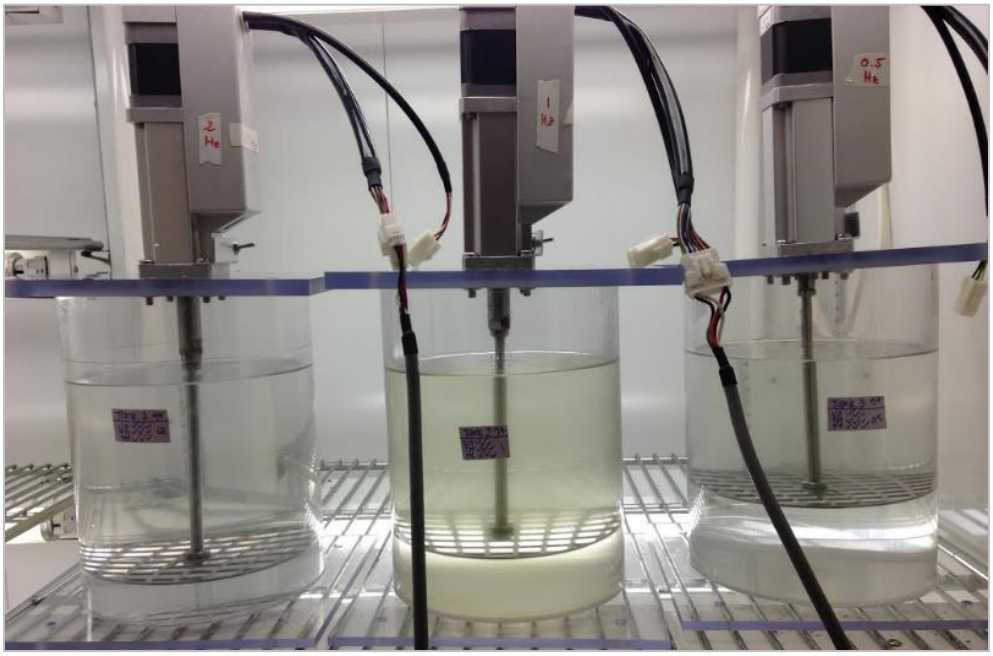

Figure 2 | Image of oscillating grid tanks in the light and temperature controlled incubator. Grids were set to oscillate at a specific frequency to generate homogenous turbulence in the tanks.

the lower part of the tank (between 20 and 70 mm above the bottom) (Figure 2). The range of oscillating frequencies used in this study (0.5 Hz – 2 Hz) produced a range of turbulent energy dissipation rates (ε = 0.02 cm^2 s^{-3} to 1.2 cm^2 s^{-3}; (Guadayol et al., 2009).

3.2 Monoculture experiments

Three diatoms (*Thalassiosira* sp.: cell length 18 – 20 µm; *Chaetoceros* sp.: cell length 14 – 16 µm; *Thalassiosira pseudonana:* cell length 6 – 8 µm*)* and one haptophyte (*Phaeocystis globosa:* cell length 4 – 7 µm) were incubated with their associated heterotrophic bacteria in oscillating grid tanks to measure cell growth and TEP formation under small-scale turbulence (Figure 3). *Thalassiosira* sp. (UNC 1203) and *Chaetoceros* sp. (UNC 1202) were isolated in

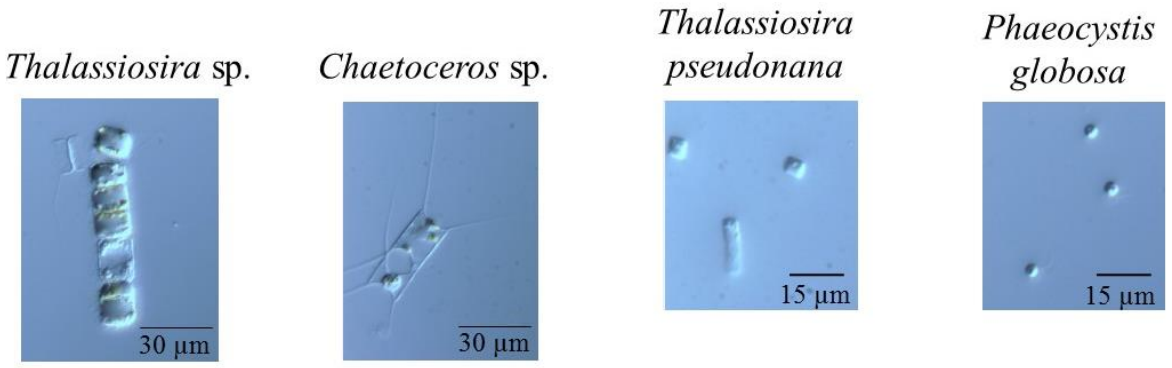

Figure 3 | Microscope images of the monocultures used in the oscillating grid incubations.

2012 from Station P8 along the Line P transect in the Northeast Pacific Ocean (Marchetti Lab, UNC – Chapel Hill). *T. pseudonana* (CCMP 1335) and *P. globosa* (CCMP 2754) were obtained from the National Center for Marine Algae and Microbiota at the Bigelow Laboratory for Ocean Sciences. Stock cultures were maintained at constant light and temperature in artificial seawater medium Aquil (Price et al., 1989). The Aquil medium recipe was amended to have 1/6 the amount of NO_3^- to ensure that the same nutrient (NO_3^-) put the all the phytoplankton cells in

stationary phase. $Si(OH)_4$ was doubled to ensure that diatom growth was not limited by silica (50 μM NO_3^-, 10 μM $PO4_3^-$, and 200 μM $Si(OH)_4$; final concentrations). Three to four tanks (varied depending on experiment) were inoculated with 8 mL of maintenance culture in mid-exponential growth and filled with 2.33 L of Aquil medium that was sterilized in a microwave for 9 min and cooled off overnight. An oscillating frequency (either 0.5 Hz, 1 Hz, 1.5 Hz, or 2 Hz) was applied to each of the tanks and kept constant throughout the time course of the experiment (Figure 4). The lowest frequency for each of the monocultures was tested prior to the incubations and represented the lowest possible mixing rate at which most of the cells stayed in suspension.

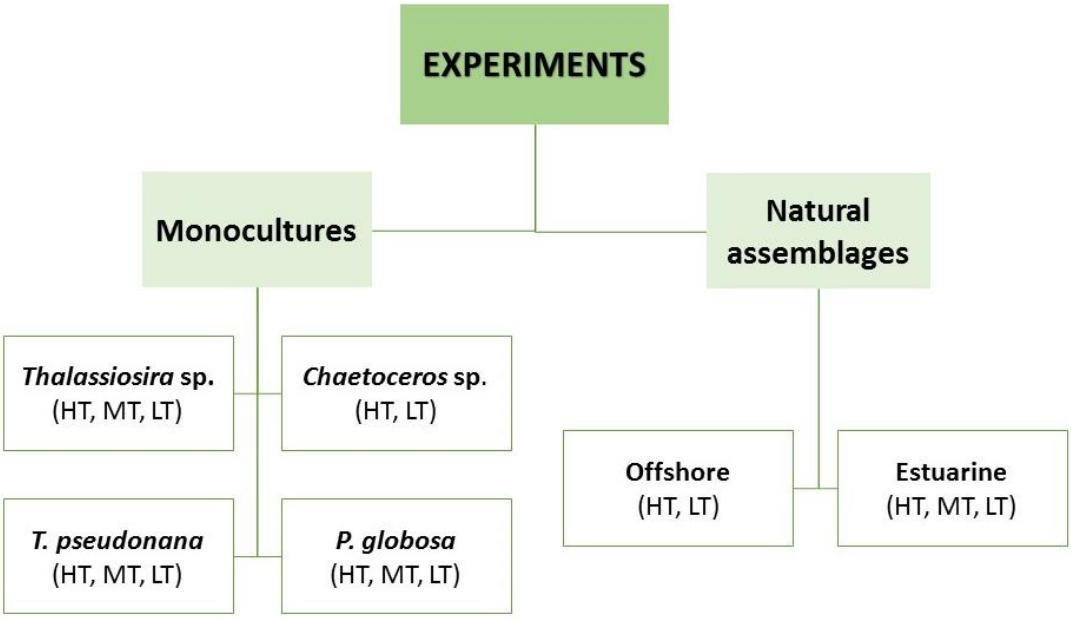

Figure 4 | Schematic depicting the six incubations in this study. Four incubations were conducted with monocultures of phytoplankton (*Thalassiosira* sp., *Chaetoceros* sp., *T. pseudonana*, and *P. globosa*) and two incubations were conducted with natural assemblages from offshore and estuarine environments. Each incubation was subjected to a range of turbulent treatments, as depicted by HT (high turbulence), MT (medium turbulence), and LT (low turbulence).

Cultures were incubated under constant light (120 – 140 μM photons m^2 s^{-1}) and temperature until the cells reached stationary growth. Following the start of the incubations, each tank was

subsampled daily to monitor *in vivo* fluorescence as a measure of algal biomass using a 10-AU Turner fluorometer (expressed as relative fluorescence units – RFU). Daily RFU readings were used to identify the different growth phases and informed when to sample tank water for analysis of phytoplankton cell abundance, dissolved inorganic nutrients, and TEP concentration as described below (see *3.4*). Length of each incubation varied depending on the growth rate of the monocultures (*Thalassiosira* sp.: 14 days, *Chaetoceros* sp.: 10 days, *T. pseudonana:* 10 days, and *P. globosa*: 10 days). Replicates of growth rates were obtained for oscillating grid incubations with *Thalassiosira* sp. (Total experiments, 2 Hz: 2; 1.5 Hz: 2; 1 Hz: 4) and *Chaetoceros* sp. (Total experiments, 2 Hz: 4; 1 Hz: 3) when every tank did not experience growth after being inoculated. When this happened in one of the tanks, daily RFU measurements were taken for the other tanks that exhibited growth. The entire suite of water analysis parameters was only collected when all three mixing tanks were inoculated with the same batch culture medium.

3.3 Natural assemblages

Effects of turbulence on TEP formation within natural assemblages were tested in two oscillating grid experiments using offshore and estuarine waters (Figure 5). The offshore experiment was conducted during *RV Endeavor* cruise 556 (April 29 – May 3, 2015) with water taken at a site in the Mid-Atlantic Bight (Figure 5, Station 08: 37°36'6.42"N, 68°24'15.90"W; water depth: 4585 m). Surface water from 25 m water depth (deep-chlorophyll maximum) and bottom water from 4500 m water depth was collected in Niskin bottles during the same CTD cast. Immediately after sampling, 5 L of bottom water was filtered through a 0.2-µm polycarbonate filter and combined with 5 L unfiltered surface water in a 10 L carboy (pre-rinsed

with 2% HCl and Milli-Q water). Surface water was diluted for two reasons: (1) to diminish effects of grazers on phytoplankton cells, and (2) to increase the amount of growth-limiting nutrients for phytoplankton during the oscillating grid experiment. Prior to initiating the experiment, the 10 L carboy was subsampled for initial concentrations (T0) of chlorophyll *a*, TEP, and dissolved nutrients (see *3.4*). Following the T0 sampling, four tanks with oscillating grids were filled to the 2 L mark and incubated at two different oscillating frequencies (duplicate tanks set to 1 Hz and 2 Hz mixing frequencies) at constant turbulence, light (100 – 120 µM photons m^2 s^{-1}), and temperature for 90 hours. Note that phytoplankton growth, as indicated by changes in chlorophyll *a*, was only measurable in two of the four tanks (i.e., one tank from each of the two turbulence treatments); therefore, only the results of the two tanks with growth are reported. The two tanks were sub-sampled for TEP, extracted chlorophyll *a*, DIN, and DIP at T0 and 24, 48, 66, and 90 hours after the incubation started. Incubation time was dictated by the length of the cruise.

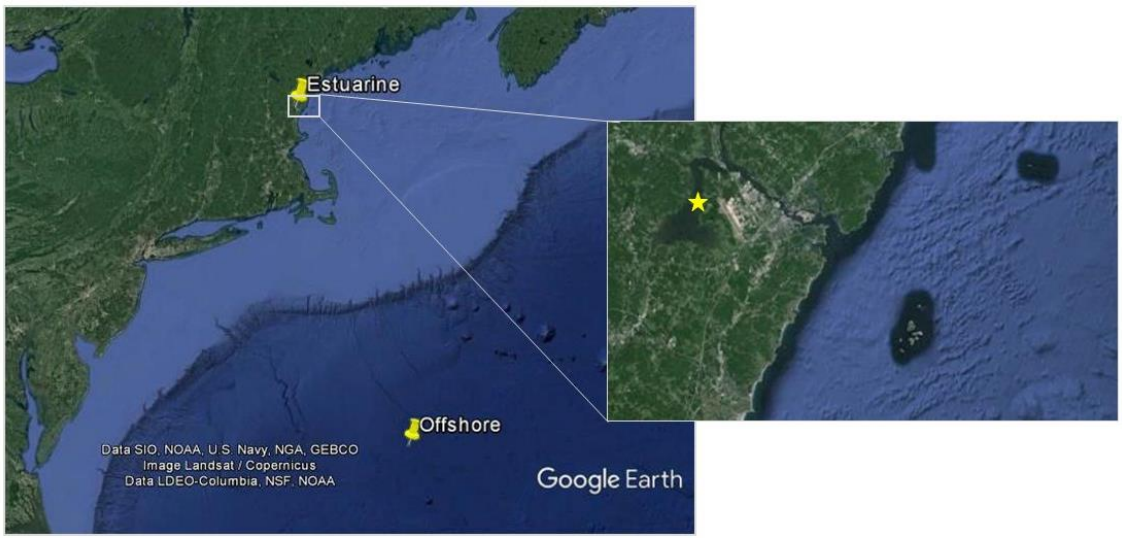

Figure 5 | Map of stations where water was taken for incubations with natural assemblages. Offshore water was collected on RV Endeavor cruise 556 (Station 08: 37°36'6.42"N, 68°24'15.90"W). The yellow star indicates where water from the Great Bay Estuary was collected at the Jackson Estuarine Laboratory (43° 5'19.68"N, 70°51'48.53"W).

The experiment with natural assemblages form the Great Bay Estuary was conducted from August 16 – August 19, 2016 using surface water sampled at low tide from the Adam's Point dock of the UNH Jackson Estuarine Laboratory (43° 5'19.68"N, 70°51'48.53"W) (Figure 5). A 10 L carboy (pre-rinsed with 10% HCl and Milli-Q water) was lowered into the surface water (19˚C) and transported back to the lab. An initial sampling was taken from the 10 L carboy and water was analyzed for chlorophyll *a*, TEP, DIN, and DIP. After an initial T0 sampling, three tanks with oscillating grids were filled to the 2.33 L mark and spiked with 30 µM NO_3^- (test experiments showed that a small NO_3^- addition was necessary to promote the growth of the phytoplankton). Oscillating frequencies were set to 2 Hz, 1 Hz, and 0.5 Hz and cells were incubated under constant turbulence, light (80 - 100 µM photons m^2 s^{-1}), and temperature for 72 hours. Tanks were sub-sampled 24, 48, and 72 hours after the experiment started for chlorophyll *a*, TEP, TIN and TIP.

3.4 Analytical methods

3.4.1 Phytoplankton and bacteria cell counts

Cell counts were obtained for the *Thalassiosira* sp. and *Chaetoceros* sp. experiments by fixing 5 mL of water with a 5% Lugol's solution (Potassium Iodide and Iodine). Samples were stored in a cool, dark drawer and 1 mL of each sample was placed on a Sedgewick rafter counting chamber and analyzed using light microscopy (Accu-scope; 300 cells or 30 fields of view for each sample). *P. globosa* cells were preserved similarly but because the 5% Lugol's solution was not pre-filtered and the small cell size, counts for all of the samples were difficult to obtain. Cell counts were obtained by light microscopy only for the first and last sampling time point in the 1 Hz tank and for the first and second sampling time point in the 0.5 Hz tank. There

is no reason to believe that the RFU per phytoplankton cell in these experiments changes with time or in the different turbulent treatments so a linear regression was applied to obtain cell concentrations for the other sampling time points ($y = 5507x - 1947$, $R^2 = 0.98$; y = cell concentration, x = RFU). For the *T. pseudonana* experiment, cell concentrations were obtained using flow cytometry (Becton Dickinson Facscalibur; fluorescence peak: 670 nm; analyzed using FloJo 7.6.1).

For both the monoculture and natural assemblages, heterotrophic bacteria counts were obtained using flow cytometry. 1 mL of water was preserved by adding 6 µL of 25% glutaraldehyde and allowed to fix in the dark for 10 minutes before being stored in -80˚C. Samples were thawed, 5 µL of 100x SYBR Green I (DNA stain) was added to 450 µL of preserved water sample, and the samples were run on a Becton Dickinson Facscalibur flow cytometer (fluorescence peak: 575 nm). Heterotrophic bacteria counts were obtained by plotting the number of cells that fluoresced at 575 nm against the side scatter of the particles using FloJo 7.6.1 Software Analysis.

3.4.2 Growth rates and phases

Intrinsic growth rates in the monocultures were obtained by plotting the natural log of daily RFU against time since inoculation (Brand et al., 1981; Monod, 1949). By examining the log of the daily RFU measurements, growth phases for each sampling time were determined for the incubations (Table 1). Based off the slopes of the log RFU curves, *Thalassiosira* sp. and *P. globosa* were in early exponential, mid-exponential, and stationary phase at the 1st, 2nd, and 3rd water samplings, respectively (Table 1). *T. pseudonana* was sampled four times and was likely in early, middle, and late exponential during the first three samples and reached stationary phase by the fourth and final water sampling (Table 1). Based on the slope of the log of RFU data for the

Chaetoceros sp. incubation, the cells were in early, middle, and late exponential growth phases at the first three sampling time points (Table 1).

Net growth rates were similarly determined for the offshore and estuarine experiments, using extracted chlorophyll *a* instead of fluorescence readings. Extracted chlorophyll *a* concentrations were obtained using the acetone extraction method (Lorenzen, 1967). For both experiments, between 50 and 800 mL of water sample was passed through GF/F filters and stored in a -20˚C freezer. Chlorophyll *a* was later extracted by putting each filter in 10 mL of 90% acetone and stored at -20˚C for 24 – 48 hours. Concentration of extracted chlorophyll was found using an equation adapted from Lorenzen (1967), $a = 0.548 \times (R_b - R_a) \times (v/V)$, by considering the volume of water filtered (V), volume of acetone used in extraction (v), fluorometer calibration to a known standard (0.548), the relative fluorescence after extraction (R_b), and relative fluorescence due to pheophytin (R_a). Log of extracted chlorophyll concentrations were plotted against time to obtain net growth rates for the experiments with natural assemblages. Net growth rates for the offshore and estuarine experiments were calculated using the log of values from T24 to T90 and T0 to T48, respectively. Phytoplankton cells in the offshore experiment were in early exponential growth at T24 and likely in mid-exponential until the final water sampling done 90 hours after the incubation (Table 3). The estuarine natural assemblages were likely in early exponential growth when the tanks were filled at T0, mid-exponential at T24, late exponential at T48, and stationary at T72 (Table 3).

3.4.3 Photosynthetic efficiency

Active fluorescence techniques were used in the *Thalassiosira* sp., *T. pseudonana,* and *P. globosa* experiments to measure the ratio of variable to maximum photochemical yield of photosystem II (F_v/F_m) (Geider et al., 1993a, 1993b). F_v/F_m was measured when the cells were in

mid-exponential growth using a Statlantic Flourescent Induction and Relaxation (FIRe) System. 5 mL of water sample was put in the dark to acclimate and the sample was excited by a weak blue light. Fluorescence was detected at wavelengths >695 nm and F_v/F_m values were calculated based on the minimum and maximum fluorescence of the dark-adapted sample.

3.4.4 Dissolved inorganic nurients

At each sampling time point, 12 mL of GF/F filtered tank water was frozen and later analyzed for dissolved inorganic nutrients using standard colorimetric methods (EPA Methods 353.2 and 365). To determine nitrate concentrations, the pre-filtered sample was run through a column with copper-cadmium, reducing the nitrate to nitrite. Next, a highly colored azo dye was added that binds to the nitrite and concentrations were quantified colorimetrically (EPA Method 353.2). Phosphorus concentrations were obtained by adding ammonium molybdate and antimony potassium tartrate to the pre-filtered sample in an acid medium. Next, the phosphorus was combined with ascorbic acid and reduced to an intensely blue-colored complex that was measured using a spectrophotometer (EPA Method 365).

Nitrogen (monocultures and natural assemblages) and phosphorus (natural assemblages only) quotas were calculated for each tank by dividing the change in nitrogen concentration in the water by change in phytoplankton cell numbers during exponential growth ($\frac{N_{t1}-N_{t2}}{C_{t2}-C_{t1}}$; N = DIN or DIP (M) and C = phytoplankton cell or chlorophyll concentration (L^{-1})). To compare values between experiments an assumption was made that the nutrient concentration change in the water was due to uptake by the phytoplankton cells.

3.4.5 Transparent exopolymer particles (TEP)

Concentration of TEP was measured colorimetrically following the procedure of (Passow and Alldredge, 1995). Cell- (monocultures) and chlorophyll- (natural assemblages) specific TEP

values were calculated by dividing TEP values by the concentration of cells or chlorophyll in the water samples. Concentrations of TEP were obtained by filtering 5 mL of water for the monocultures and 20 - 50 mL of water for the natural assemblages onto 0.4 μm polycarbonate filters (analytical triplicates) that were subsequently stained with 0.5 mL Alcian Blue (AB) working solution. The pH of AB working solution was buffered with HCl to have a pH of 2.5 and pre-filtered through a 0.2 μm acro-disk. Buffering the working solution is done because the carbon chains that make up TEP are acid polysaccharides and if the pH is too high the AB cannot stain the TEP carbon matrices. After adding AB stain, the filters were rinsed with Milli-Q and stored in -20˚C. To prepare the filters for light intensity readings on the spectrophotometer, they were submerged in 5 mL 80% Sulfuric Acid for ~2 hours and gently agitated every 30 minutes to mix well. Intensity of the blue absorbance (787 nm) was measured using a Milton Roy Spectrophotometer 601-1984.

The dye solution was calibrated by making a homogenous solution of Xanthan Gum (XG, polysaccharide) and creating a dilution curve. 1 – 5 mL of XG solution was filtered onto pre-weighed 0.4 μm polycarbonate filters. The 5 filters of each volume filtered (analytical replicates) were placed in an oven (50˚C – 70˚C) for 12 to 24 hours and weighed to find the amount of XG on the filters at each dilution volume. 5 filters of each volume filtered (analytical replicates) were stained with AB working solution, rinsed with Milli-Q, and stored in -20˚C. The filters with AB stain were prepped and analyzed using the same methods described above. The mass of XG on each filter was plotted against blue absorbance for the corresponding filters that were stained with AB. The slope of the line was then applied to the absorbance values obtained in the experiments and TEP concentrations are expressed as XG equivalents.

An additional set of AB stained filters from the *Thalassiosira* sp., *T. pseudonana*, and *P. globosa* experiments were prepared for microscopic analysis using CytoClear slides (Long and Azam, 1996). 10 to 15 mL of sample water was filtered onto 0.4 μm isopore membrane filters, stained with AB, rinsed with Milli-Q, and placed on a frosted slide. A drop of oil was added and a cover slip placed on top of the filter. Slides were stored in 4˚C and pictures were taken using an Accu-scope and bright field microscopy.

4. Results

4.1 Growth Conditions under turbulence

***Thalassiosira* sp.**

Thalassiosira sp. cell concentrations increased throughout the incubation (Figure 6). Initial cell concentrations in the high, medium, and low turbulence tanks were 0.05×10^7 cells L^{-1}, 0.07×10^7 cells L^{-1}, and 0.10×10^7 cells L^{-1}, respectively (Figure 6 and Table 2). From the first to second sampling time point cell concentration increased by a factor of 22 in the high mixing tank and ~15 in the medium and low mixing tanks. At the third and final sampling time point cell concentrations were 2.8×10^7 cells L^{-1} (2 Hz), 3.3×10^7 cells L^{-1} (1.5 Hz), and 3.5×10^7 cells L^{-1} (1 Hz). Growth rates were 0.38 day^{-1}, 0.41 day^{-1}, and 0.42 day^{-1} for the high, medium, and low turbulence tanks, respectively (Table 1). F_v/F_m values were 0.6 for all three tanks (Table 1). From the first to third sampling, heterotrophic bacteria cells increased by a factor of 3 in the high mixing tank and ~11 in the medium and low mixing tanks (Table 2).

Levels of DIN decreased throughout the experiment; nitrogen cell quotas were 5.2 pM N cell $^{-1}$ in the highest mixing tank and thus 1.2 and 4.7 times higher compared to those in the 1.5 Hz (4.3 pM N cell $^{-1}$) and 1 Hz (1.1 pM N cell $^{-1}$) mixing tanks (Figure 7 and Table 1).

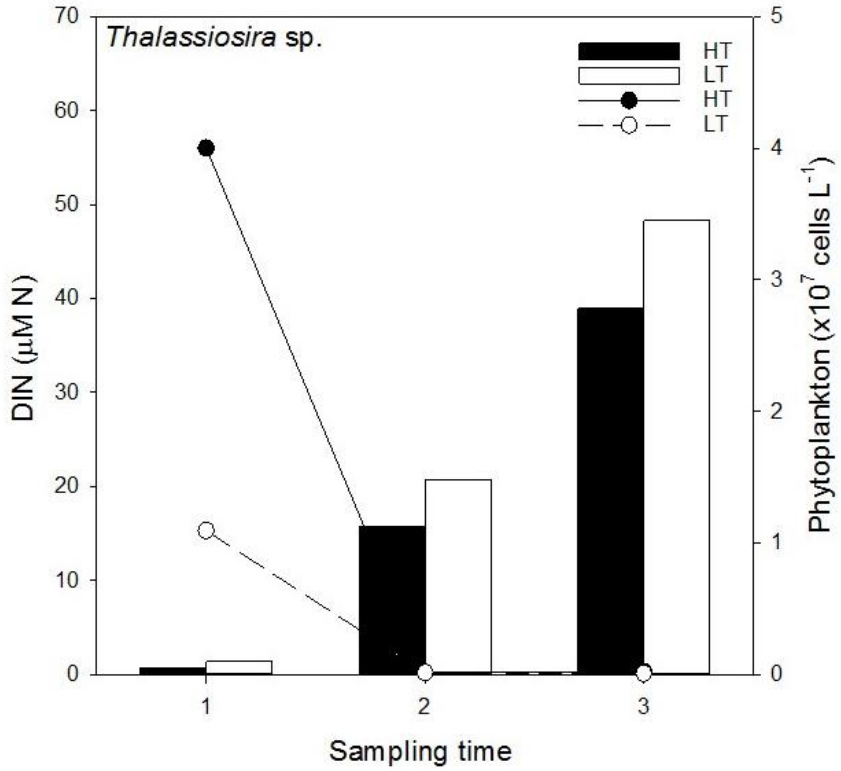

Figure 6 | Dissolved inorganic Nitrogen (DIN) concentrations (primary y-axis, scatter plot) and phytoplankton cell concentrations (secondary y-axis, bar graph) at the three sampling time points (x-axis) for the *Thalassiosira* sp. monoculture incubation. HT (solid bars and solid circles) means high turbulent tanks and LT (white bars and white circles) means low turbulent tanks.

Chaetoceros sp.

Cell concentrations increased in both high and low mixing tanks throughout the incubation (Figure 8). At the first sampling time point, there were 0.7×10^7 cells L^{-1} and 1.0×10^7 cells L^{-1} in the 2 Hz and 1 Hz tanks, respectively (Figure 8 and Table 2). From the first to second sampling, cell concentrations increased by a factor of about 6.5 in both tanks. At the final sampling, there were 8.2×10^7 cells L^{-1} (2 Hz) and 10.0×10^7 cells L^{-1} (1 Hz) in the tanks. Growth

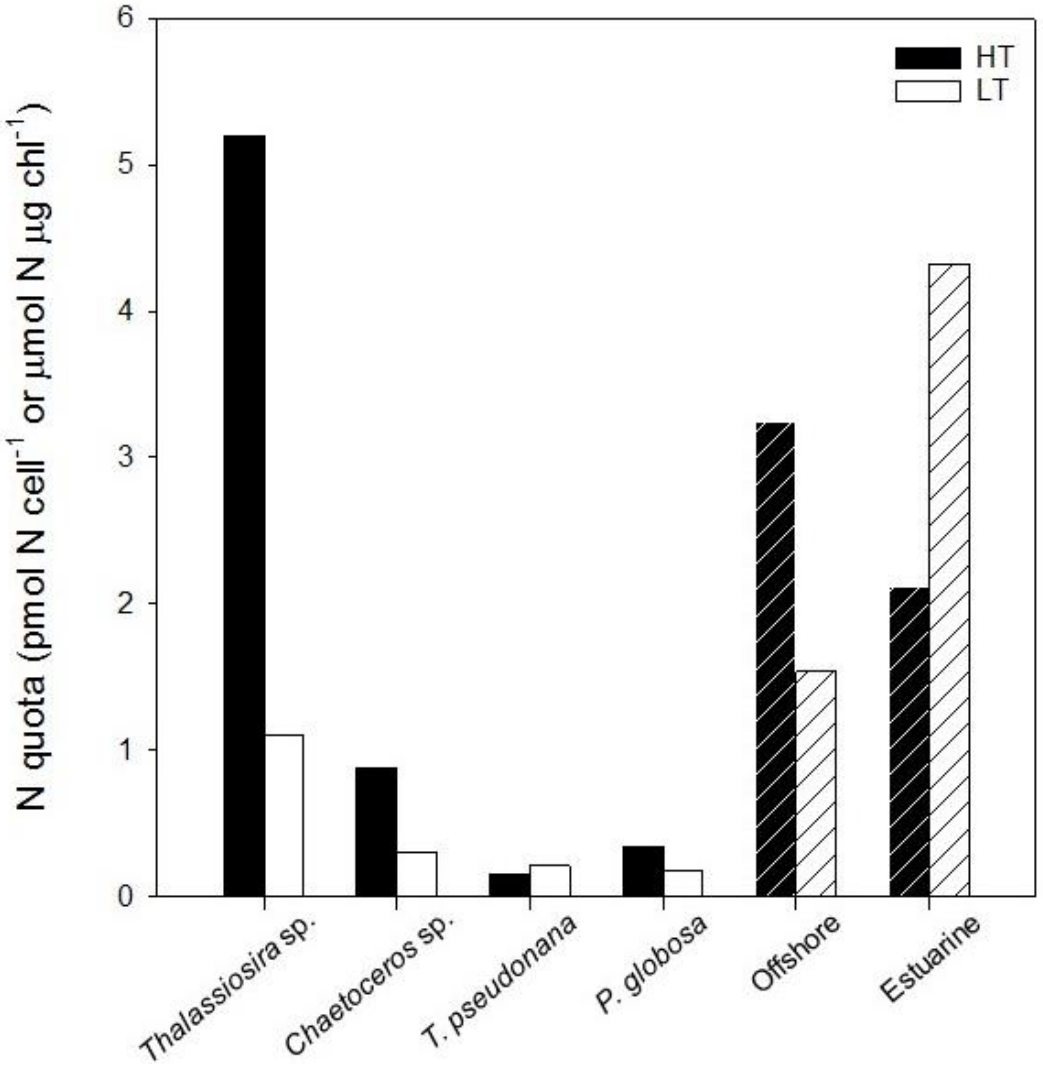

Figure 7 | Nitrogen cell quotas for monocultures (solid bars) and natural assemblages (striped bars). HT (black) stands for high turbulent tanks and LT (white) stands for low turbulent tanks.

rates were 0.97 day^{-1} and 0.94 day^{-1} for in 2 and 1 Hz mixing tanks, respectively (Table 1). From the first to third sampling, heterotrophic bacteria cells increased by a factor of about 12 in the high mixing tank and about 10 in the low mixing tank (Table 2).

DIN levels decreased throughout the incubation in both tanks, and the nitrogen cell quota in the higher mixing tank (0.88 pM N cell $^{-1}$) was about 3 times higher compared to the 1 Hz tank (0.30 pM N cell $^{-1}$) (Figure 7 and Table 1).

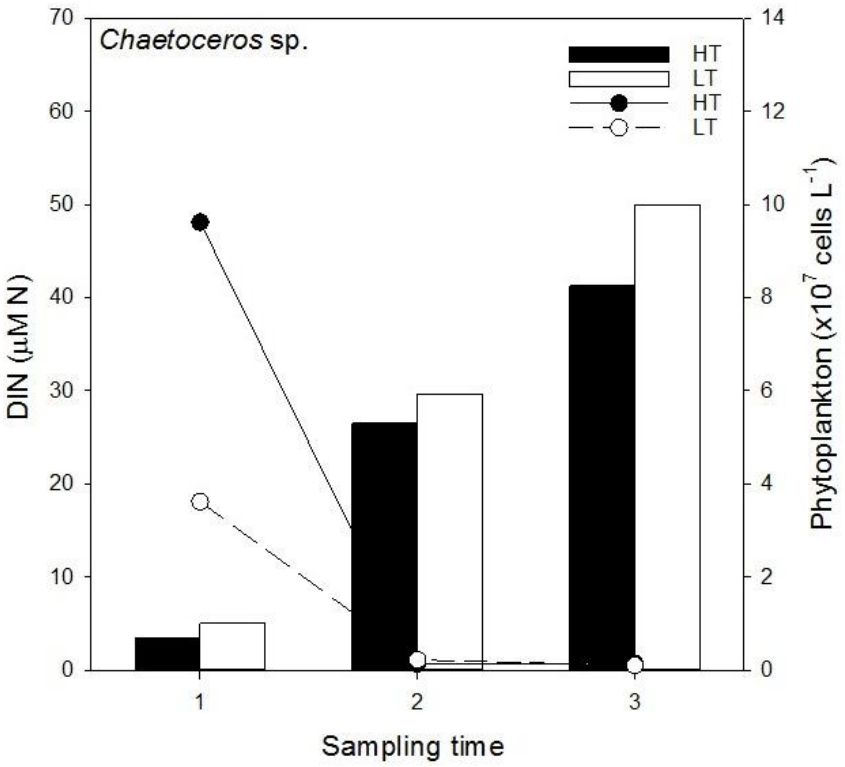

Figure 8 | Dissolved inorganic Nitrogen (DIN) concentrations (primary y-axis, scatter plot) and phytoplankton cell concentrations (secondary y-axis, bar graph) at the three sampling time points (x-axis) for the *Chaetoceros* sp. monoculture incubation. HT (solid bars and solid circles) means high turbulent tanks and LT (white bars and white circles) means low turbulent tanks.

Thalassiosira pseudonana

Cell concentrations increased in the high, medium, and low mixing tank throughout the incubation (Figure 9). Initial cell numbers were 1.3×10^7 cells L^{-1} (2 Hz), 0.9×10^7 cells L^{-1} (1 Hz), and 6.2×10^7 cells L^{-1} (0.5 Hz) (Figure 9 and Table 2); in the 2 Hz and 1 Hz mixing tanks, diatom cells increased between the first and second time point by a factor of about 8.5; at the same time cell concentrations in the lower mixing tank stayed constant. Final cell concentrations at the third sampling time point were 29.7×10^7 cells L^{-1}, 30.4×10^7 cells L^{-1}, and 28.3×10^7 cells L^{-1} in the 2, 1, and 0.5 Hz mixing tanks, respectively (Figure 9 and Table 2). Growth rates were 1.02 day^{-1} (2 Hz), 1.02 day^{-1} (1 Hz), and 0.99 day^{-1} (0.5 Hz) for the three tanks (Table 1). F_v/F_m values were 0.6 for all three tanks (Table 1). From the first to third sampling time point heterotrophic

Table 1 Experimental conditions and results from monoculture incubations with *Thalassiosira* sp., *Chaetoceros* sp., *T. pseudonana*, and *P. globosa*. Reported values for cell length, dissipation rate, oscillating frequency, intrinsic growth rate, nitrogen cell quota, photosynthetic efficiency, and sampling time/growth phase. Growth phases are EE: early-exponential, ME: mid-exponential, LE: late-exponential, and S: stationary (see text for more details).

	Cell length (µm)	Dissipation rate, ε ($cm^2\ s^{-3}$)	Oscillating frequency (Hz)	Intrinsic growth rate (day^{-1})	N quota (pmol N $cell^{-1}$)	Photosynthetic efficiency (F_v/F_m)	Sampling time/growth phase
Thalassiosira sp.	18 – 20	1.20	2.0	0.38	5.2	0.6	1/EE 2/ME 3/S
		0.52	1.5	0.41	4.3	0.6	1/EE 2/ME 3/S
		0.16	1.0	0.42	1.1	0.6	1/EE 2/ME 3/S
Chaetoceros sp.	14 – 16	1.20	2.0	0.97	0.88	-	1/EE 2/ME 3/LE
		0.16	1.0	0.94	0.30	-	1/EE 2/ME 3/LE
T. pseudonana	6 – 8	1.20	2.0	1.02	0.15	0.6	1/EE 2/ME 3/LE 4/S
		0.16	1.0	1.02	0.09	0.6	1/EE 2/ME 3/LE 4/S
		0.02	0.5	0.99	0.21	0.6	1/EE 2/ME 3/LE 4/S
P. globosa	4 - 7	1.20	2.0	0.79	0.34	0.5	1/EE 2/ME 3/S
		0.16	1.0	0.80	0.23	0.5	1/EE 2/ME 3/S
		0.02	0.5	0.75	0.18	0.5	1/EE 2/ME 3/S

bacteria increased by a factor of ~9 in all three mixing tanks (Figure 9 and Table 2).

Levels of DIN decreased in the surrounding water throughout the experiments in all three tanks and nitrogen cell quotas were 0.15 pM N cell $^{-1}$, 0.09 pM N cell $^{-1}$, and 0.21 pM N cell $^{-1}$ for the high, medium, and low mixing tanks, respectively (Figure 7 and Table 1).

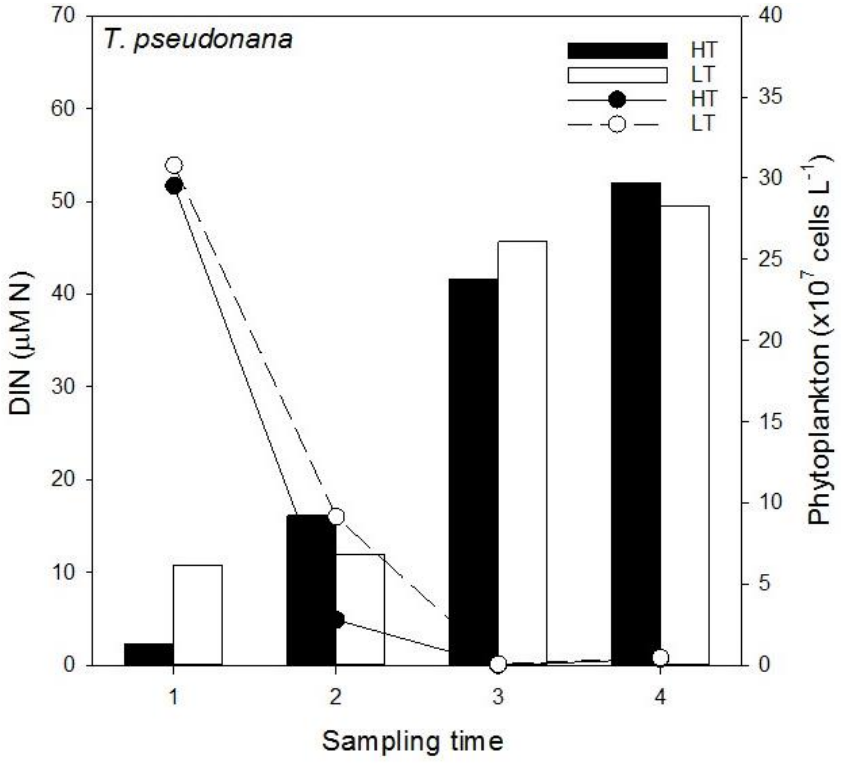

Figure 9 | Dissolved inorganic Nitrogen (DIN) concentrations (primary y-axis, scatter plot) and phytoplankton cell concentrations (secondary y-axis, bar graph) at the four sampling time points (x-axis) for the *T. pseudonana* monoculture incubation. HT (solid bars and solid circles) means high turbulent tanks and LT (white bars and white circles) means low turbulent tanks.

Phaeocystis globosa

Cell concentrations at the first sampling time point were 0.6×10^7 cells L^{-1}, 1.30×10^7 cells L^{-1}, and 0.90×10^7 cells L^{-1} for the high, medium, and low mixing tanks, respectively (Figure 10 and Table 2). In the high and low mixing tanks, cell concentrations increased from the first to second time point by a factor of about 17; at the same time, cell counts increased by a factor of 9

in the 1 Hz mixing tank (Table 2). Cell concentrations at the last time point were 26.7×10^7 cells L^{-1}, 23.9×10^7 cells L^{-1}, and 28.4×10^7 cells L^{-1} in the high, medium, and low mixing tanks, respectively (Table 2). Growth rates were 0.79 day^{-1} (2 Hz), 0.80 day^{-1} (1 Hz), and 0.75 day^{-1} (0.5 Hz) (Table 1). F_v/F_m values were 0.5 for all three tanks 9 (Table 1). In the high mixing tank, heterotrophic bacteria increased by a factor of ~3 over the course of the incubation; at the same time, heterotrophic bacteria did not increase in the 1 Hz and 0.5 Hz tanks (Table 2).

DIN concentration decreased throughout the incubations and nitrogen quotas were 0.34 pM N cell $^{-1}$ (2 Hz), 0.23 pM N cell $^{-1}$ (1 Hz), and 0.18 pM N cell $^{-1}$ (0.5 Hz) (Figure 7 and Table 1).

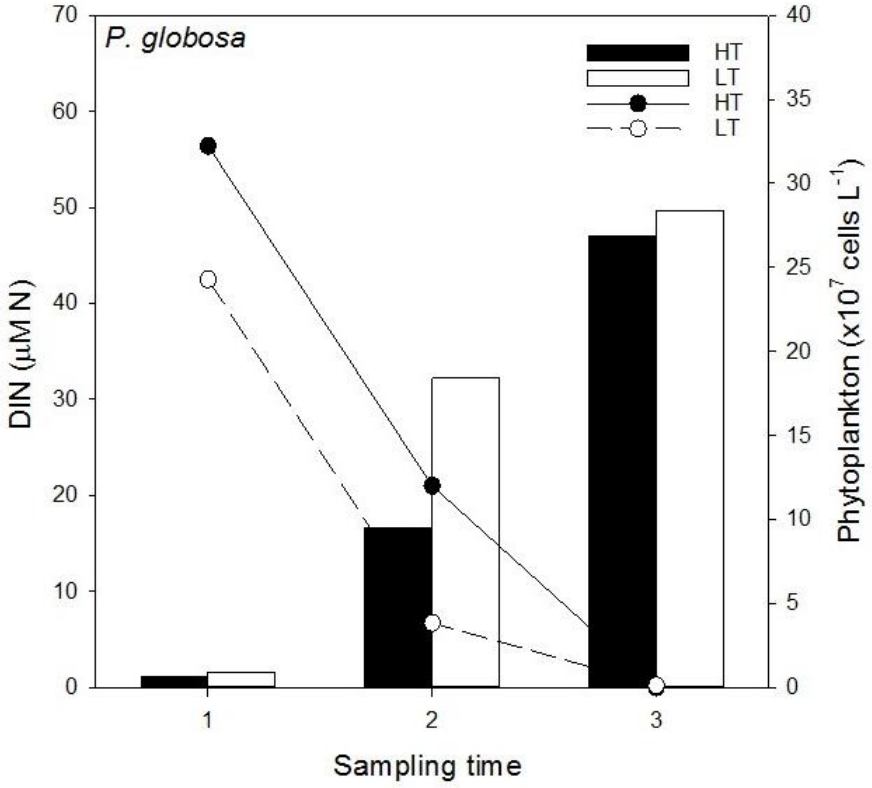

Figure 10 | Dissolved inorganic Nitrogen (DIN) concentrations (primary y-axis, scatter plot) and phytoplankton cell concentrations (secondary y-axis, bar graph) at the three sampling time points (x-axis) for the *P. globosa* monoculture incubation. HT (solid bars and solid circles) means high turbulent tanks and LT (white bars and white circles) means low turbulent tanks.

Table 2 Results from monoculture incubations with *Thalassiosira* sp., *Chaetoceros* sp., *T. pseudonana*, and *P. globosa*. Reported values for oscillating frequency, sampling time, phytoplankton cell number, bacterial cell number, volumetric TEP, cell-specific TEP, and DIN.

	Oscillating frequency (Hz)	Sampling time	Phytoplankton cell number ($\times 10^7$ cells L^{-1})	Bacteria cell number ($\times 10^9$ cells L^{-1})	TEP (µg XG equiv. L^{-1})	TEP/cell (pg XG equiv. $cell^{-1}$)	DIN (µM)
Thalassiosira sp.	2.0	1	0.05	1.1	267 ± 18	498 ± 34	56.0
		2	1.1	5.2	755 ± 53	67 ± 5	0.2
		3	2.8	3.3	683 ± 8	25 ± 0.3	0.3
	1.5	1	0.07	1.2	226 ± 96	327 ± 138	44.7
		2	1.1	2.6	723 ± 69	65 ± 6	0.2
		3	3.3	11.2	672 ± 30	22 ± 1	0.4
	1.0	1	0.1	1.1	288 ± 62	294 ± 65	15.3
		2	1.5	6.9	697 ± 99	47 ± 7	0.2
		3	3.5	11.7	670 ± 22	19 ± 1	0.1
Chaetoceros sp.	2.0	1	0.7	5.1	529 ± 51	77 ± 7	41.2
		2	5.3	0.6	731 ± 77	14 ± 2	0.6
		3	8.2	12.4	1142 ± 69	19 ± 1	0.6
	1.0	1	1.0	0.7	495 ± 25	49 ± 3	15.5
		2	5.9	0.6	680 ± 155	11 ± 3	0.9
		3	10.0	18.3	1146 ± 130	19 ± 2	0.4
Thalassiosira pseudonana	2.0	1	1.3	1.6	110 ± 34	8.3 ± 2.5	44.3
		2	9.2	3.7	113 ± 19	1.2 ± 0.2	4.2
		3	23.7	4.6	442 ± 111	1.9 ± 0.5	0.0
		4	29.7	9.2	647 ± 160	2.2 ± 0.6	0.6
	1.0	1	0.9	1.0	140 ± 47	15.8 ± 5.3	26.8
		2	8.8	2.9	147 ± 20	1.7 ± 0.2	14.4
		3	26.0	4.8	380 ± 69	1.5 ± 0.3	0.2
		4	30.4	9.9	870 ± 140	2.9 ± 0.5	0.9
	0.5	1	6.2	1.7	139 ± 48	2.2 ± 0.8	46.2
		2	6.8	2.1	174 ± 21	2.6 ± 0.3	13.7
		3	26.1	4.7	283 ± 48	1.1 ± 0.2	0.1
		4	28.3	8.8	672 ± 90	2.4 ± 0.3	0.7
Phaeocystis globosa	2.0	1	0.62	3.2	317 ± 41	50.8 ± 6.6	48.3
		2	9.5	4.4	309 ± 10	3.2 ± 0.1	18.0
		3	26.9	8.6	518 ± 30	1.9 ± 0.1	0.0
	1.0	1	1.3	1.9	275 ± 23	21.1 ± 1.7	41.9
		2	11.9	2.0	269 ± 26	2.3 ± 0.2	17.5
		3	23.9	2.2	209 ± 11	0.9 ± 0.1	0.0
	0.5	1	0.89	3.2	258 ± 12	28.8 ± 1.3	36.5
		2	18.3	3.9	334 ± 34	1.8 ± 0.2	5.7
		3	28.4	3.3	523 ± 26	1.8 ± 0.1	0.1

Offshore natural assemblages

Levels of chlorophyll *a* increased in the two tanks throughout the 90 hours incubation by a factor of 8 (2 Hz) and 5 (1 Hz), reaching 3.5 µg L^{-1} (2 Hz) and 2.3 µg L^{-1} (1 Hz) at the end of the experiment (Figure 11). Changes in chlorophyll *a* over time resulted in net growth rates of 1.19 day^{-1} (2 Hz) and 1.43 day^{-1} in the high and low mixing tank, respectively (Table 3). Bacteria cell numbers increased by a factor of ~12 and ~6 from T0 to T90 in the high and low mixing tanks, respectively (Table 4).

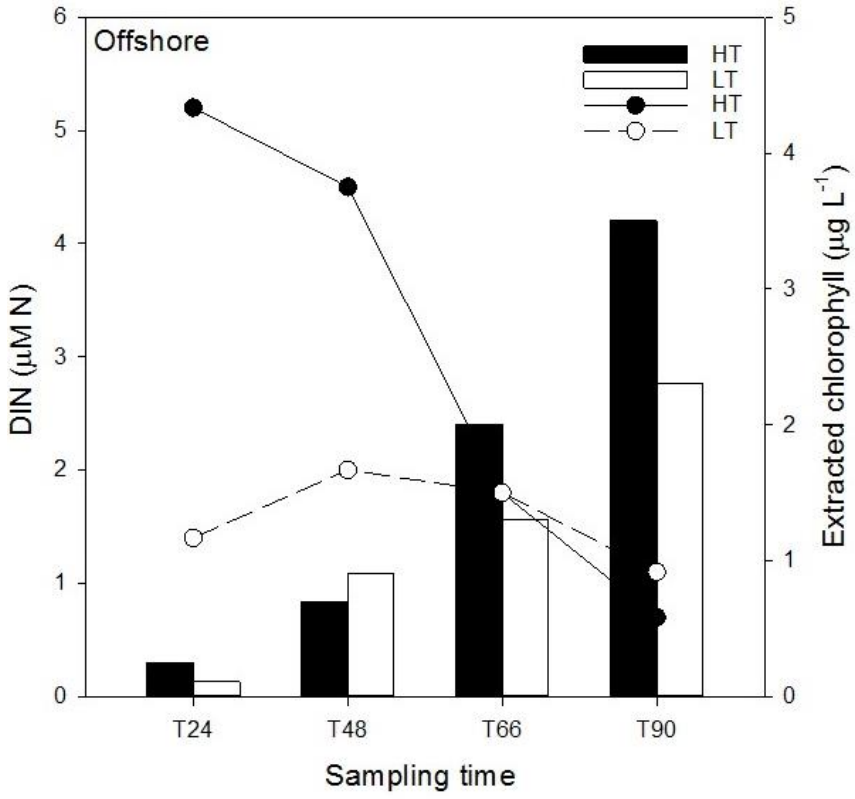

Figure 11 | Dissolved inorganic Nitrogen (DIN) concentrations (primary y-axis, scatter plot) and extracted chlorophyll concentrations (secondary y-axis, bar graph) at the four sampling time points (x-axis) for the offshore incubation. HT (solid bars and solid circles) means high turbulent tanks and LT (white bars and white circles) means low turbulent tanks.

Table 3 Experimental conditions and results from incubations with offshore and estuarine natural assemblages. Reported values for dissipation rate, oscillating frequency, net growth rate, nitrogen quota per chlorophyll, phosphorus quota per chlorophyll, sampling time/growth phase. Growth phases are EE: early-exponential, ME: mid-exponential, LE: late-exponential, and S: stationary (see text for more details).

	Dissipation rate, ε (cm^2 s^{-3})	Oscillating frequency (Hz)	Net growth rate (day^{-1})	N quota (µmol N µg chl^{-1})	P quota (µmol P µg chl^{-1})	Sampling time/growth phase
Offshore	1.20	2.0	1.19	1.35	0.13	T0 T24/EE T48/ME T66/ME T90/ME
	0.16	1.0	1.43	0.64	0.12	T0 T24/EE T48/ME T66/ME T90/LE
Estuarine	1.20	2.0	0.94	0.88	0.01	T0/EE T24/ME T48/LE T72/S
	0.16	1.0	0.69	0.94	0.04	T0/EE T24/ME T48/LE T72/S
	0.02	0.5	0.52	1.83	0.07	T0/EE T24/ME T48/LE T72/S

DIN concentrations decreased throughout the incubation in both the 2 and 1 Hz oscillating grid tanks from 5.1 ± 3.6 µM N at the initial sampling to 0.7 µM N and 1.1 µM N in the 2 and 1 Hz mixing tanks, respectively, at the end of the incubation (Figure 11 and Table 4). chlorophyll $^{-1}$ (1 Hz) (Table 3). Nitrogen quotas per µg chlorophyll between T48 and T90 were 1.35 µmol N µg chlorophyll $^{-1}$ (2 Hz) and 0.64 µmol N µg chlorophyll $^{-1}$ (1 Hz) (Figure 7 and Table 3). Levels of DIP decreased throughout the incubation in both tanks and was 0.91 ± 0.05

µM P at the T0 sampling and 0.02 µM P (2 Hz) and 0.21 µM P (1 Hz) at T90 (Table 4). Phosphorus quotas per µg chlorophyll between T48 and T90 were 0.13 µmol P µg chlorophyll $^{-1}$ (2 Hz) and 0.12 µmol P µg

Estuarine natural assemblages

Chlorophyll *a* concentration was 6.7 ± 0.2 µg L^{-1} in the bulk water; highest chlorophyll *a* concentrations in all three tanks were found at T48 (2 Hz: 43.9 ± 5.0 µg L^{-1}; 1 Hz: 26.6 ± 1.9 µg L^{-1}; 0.5 Hz: 18.8 ± 1.2 µg L^{-1}) (Figure 12 and Table 4). Between T48 and T72 chlorophyll *a* concentrations decreased by ~50% in all three tanks (Figure 12 and Table 4). Net growth rates

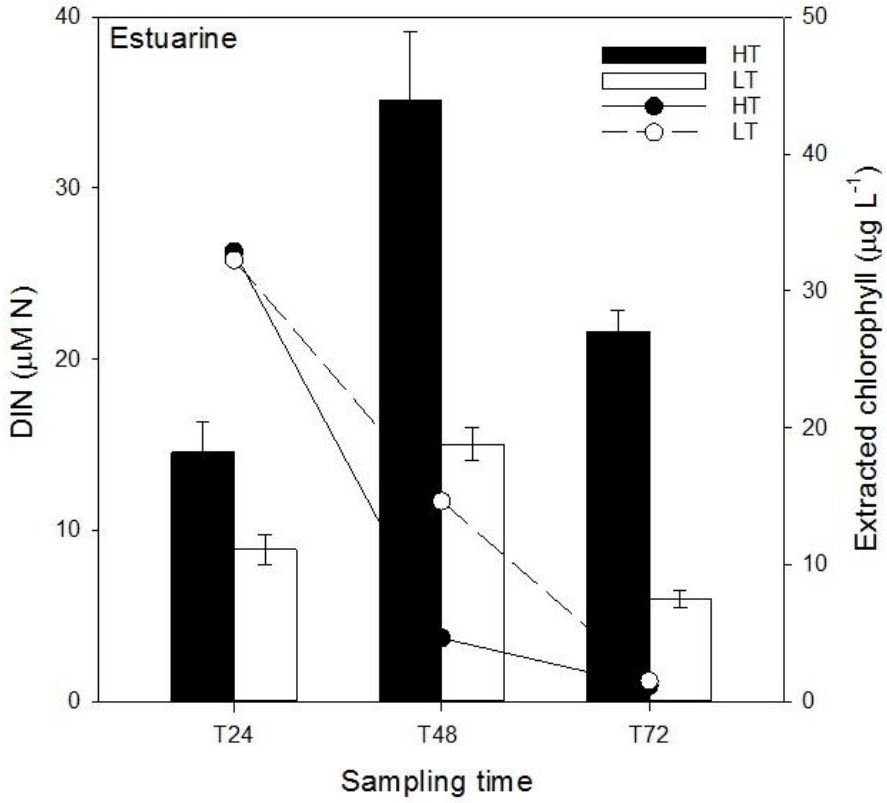

Figure 12 | Dissolved inorganic Nitrogen (DIN) concentrations (primary y-axis, scatter plot) and extracted chlorophyll concentrations (secondary y-axis, bar graph) at the three sampling time points (x-axis) for the estuarine incubation. HT (solid bars and solid circles) means high turbulent tanks and LT (white bars and white circles) means low turbulent tanks. Error bars are analytical triplicates at each sampling time point.

from T0 to T48 were 0.94 day^{-1} (2 Hz), 0.69 day^{-1} (1 Hz), and 0.52 day^{-1} (0.5 Hz) (Table 3). Heterotrophic bacteria decreased from the initial T0 sampling ($3.5 \pm 0.5 \times 10^9$ cells L^{-1}) to the T72 sampling time point (2.3×10^9 cells L^{-1}) (Table 4). In the medium and low mixing tank, bacteria cell counts stayed relatively the same from the first to final sampling time point (Table 4).

Initial DIN concentration in the bulk water before starting the incubation was 1.2 ± 0.25 µM N (Figure 12 and Table 4). To promote phytoplankton growth each tank was spiked with 30 µM NO_3^-. DIN decreased in all three tanks throughout the incubation and the concentrations were 0.9 µM N (2 Hz), 1.0 µM N (1 Hz), and 1.2 (0.5 Hz) at T72 (Figure 12 and Table 4). Nitrogen quotas per µg chlorophyll from T24 to T48, were 0.88 µmol N µg $chlorophyll^{-1}$ (2 Hz), 0.94 µmol N µg $chlorophyll^{-1}$ (1 Hz), and 1.8 µmol N µg $chlorophyll^{-1}$ for the lowest mixing tank (Figure 7 and Table 3). DIP levels decreased throughout the experiment from 1.39 µM P at T0 to 0.07 µM P (2 Hz), 0.04 µM P (1 Hz), and 0.06 µM P (0.5 Hz) at T72 (Table 4). Phosphorus quotas per µg chlorophyll between T48 and T90 were 0.014 µmol P µg $chlorophyll^{-1}$ (2 Hz), 0.042 µmol P µg $chlorophyll^{-1}$ (1 Hz), and 0.066 µmol P µg $chlorophyll^{-1}$ (0.5 Hz) (Table 3).

Table 4 Results from incubations with offshore and estuarine natural assemblages. Reported values for oscillating frequency, sampling time, extracted chlorophyll *a* (chl *a*), bacteria cell number, volumetric TEP, cell-specific TEP, DIN, and DIP. Note that the first sampling, T0, was taken from a bulk water sample before filling the tanks.

	Oscillating frequency (Hz)	Sampling time	Chl a (µg L^{-1})	Bacteria cell number ($\times 10^9$ cells L^{-1})	TEP (µg XG equiv. L^{-1})	TEP/cell (µg XG equiv. µg chl^{-1})	DIN (µM)	DIP (µM)
Offshore	2.0	T0	0.45 ± 0.11	0.05 ± 0.0	255 ± 38	564 ± 85	5.1 ± 3.6	0.91 ± 0.05
		T24	0.25	0.07	-	-	5.2	0.43
		T48	0.70	-	251 ± 27	177 ± 19	4.5	0.38
		T66	2.00	0.53	358 ± 88	223 ± 55	1.8	0.27
		T90	3.46	0.58	425 ± 160	262 ± 97	0.7	0.02
	1.0	T0	0.45 ± 0.11	0.05 ± 0.0	255 ± 38	564 ± 85	5.1 ± 3.6	0.91 ± 0.05
		T24	0.11	0.13	-	-	1.4	0.47
		T48	0.91	-	294 ± 21	182 ± 13	2.0	0.38
		T66	1.30	0.58	457 ± 53	288 ± 33	1.8	0.29
		T90	2.35	0.32	374 ± 170	219 ± 101	1.1	0.21
Estuarine	2.0	T0	7 ± 0.2	3.5 ± 0.5	162 ± 58.6	24.2 ± 8.3	-	1.39 ± 0.14
		T24	18 ± 2	3.1	322 ± 156	18.6 ± 11.1	26.3	0.40
		T48	44 ± 5	3.2	485 ± 49	11.2 ± 2.2	3.7	0.28
		T72	27 ± 2	2.3	287 ± 42	10.7 ± 2.2	0.9	0.04
	1.0	T0	7 ± 0.2	3.5 ± 0.5	162 ± 59	24.2 ± 8.3	-	1.39 ± 0.14
		T24	14 ± 2	2.8	110 ± 85	7.3 ± 4.9	21.9	0.61
		T48	27 ± 2	3.7	180 ± 21	6.8 ± 1.0	10.4	0.33
		T72	14 ± 1	3.5	222 ± 45	16.0 ± 3.2	1.0	0.09
	0.5	T0	7 ± 0.2	3.5 ± 0.5	162 ± 59	24.2 ± 8.3	-	1.39 ± 0.14
		T24	11 ± 1	2.7	157 ± 54	14.3 ± 5.6	25.8	0.62
		T48	19 ± 1	2.8	172 ± 58	9.2 ± 3.2	11.7	0.13
		T72	8 ± 1	4.0	218 ± 61	29.7 ± 10.7	1.2	0.11

4.2 Phytoplankton metabolism (TEP) under varying turbulence

***Thalassiosira* sp.**

Volumetric TEP increased between the first and the second time point by a factor of 3 (2 Hz, 1.5 Hz) and 2.4 (1 Hz), reaching 755 ± 53 µg XG equiv. L^{-1}, 723 ± 69 µg XG equiv. L^{-1}, and 697 ± 99 µg XG equiv. L^{-1} in the high, medium and low mixing tank, respectively (Table 2).

Changes between the second and the last time point were minor (2 Hz: 683 ± 8.2 µg XG equiv. L^{-1}; 1.5 Hz: 672 ± 30 µg XG equiv. L^{-1}; 1 Hz:670 ± 22 µg XG equiv. L^{-1}) (Table 2).

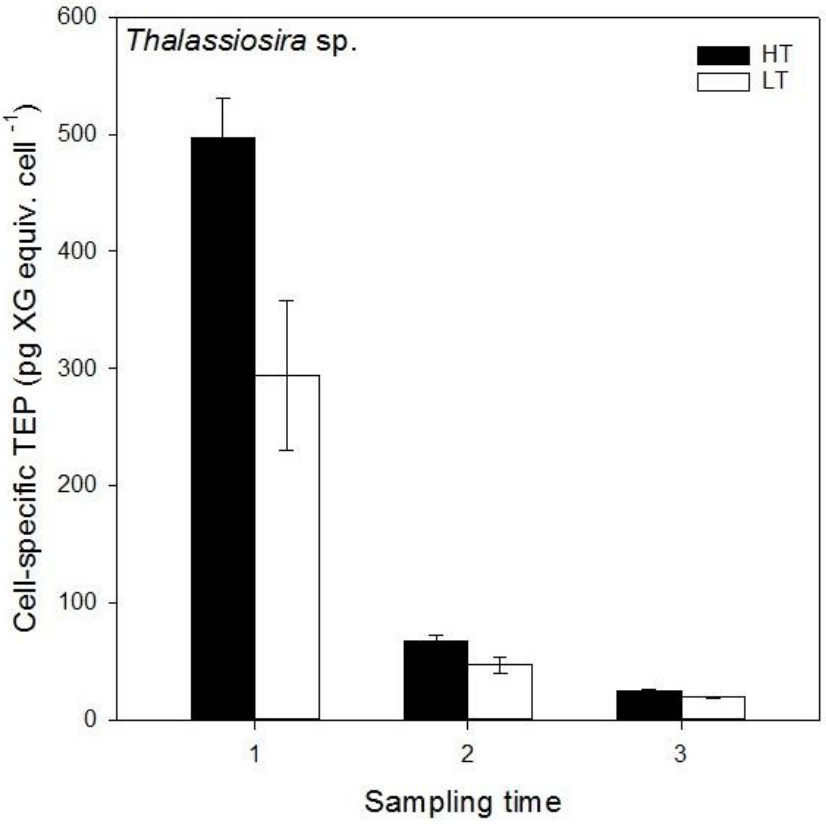

Figure 13 | Cell-specific TEP for the *Thalassiosira* sp. monoculture incubation. HT (solid bars) stands for high turbulent tanks and LT (white bars) stands for low turbulent tanks. Numbers on the x-axis indicate the sampling time point. Error bars are analytical replicates at each sampling time point.

Highest cell-specific TEP in all three tanks was found at the first time point when TEP per cell was about 1.5 times higher in the higher turbulence tank than the other two tanks (2 Hz: 497 ± 33.5 pg XG equiv. cell $^{-1}$; 1.5 Hz: 327 ± 138 pg XG equiv. cell $^{-1}$; 1 Hz: 294 ± 64 pg XG equiv. cell $^{-1}$) (Figure 13 and Table 2). In the higher mixing tank, values decreased by a factor of 7 from the first to the second time point; at the same time values decreased by a factor of about 5 and 6 in the medium and low mixing tank, respectively (Table 2). Cell-specific TEP in all three

tanks was lowest at the end of the incubation, ranging between 19 ± 0.7 pg XG equiv. cell $^{-1}$ and 25 ± 0.3 pg XG equiv. cell $^{-1}$ (Figure 13 and Table 2).

Chaetoceros sp.

Volumetric TEP levels at the first and second time point in both high and low mixing tanks were similar; volumetric TEP in both tanks doubled between the second and the third time point, reaching 1142 ± 69 µg XG equiv. L^{-1} and 1146 ± 130 µg XG equiv. L^{-1} in the high and low mixing tanks, respectively (Table 2).

In both the high and low mixing tanks, cell-specific TEP concentrations were highest during the first sampling time point and decreased throughout the experiment (Figure 14 and Table 2). Initial levels of cell-specific TEP in the 2 Hz tank were 1.6 times that of the 1 Hz mixing tank (2 Hz: 77 ± 7.4 pg XG equiv. cell $^{-1}$; 1 Hz: 48.9 ± 2.5 pg XG equiv. cell $^{-1}$) (Figure 14 and Table 2); in both tanks, TEP per cell decreased by about 80% between the first and second time point, and slightly increased again towards the third time point (2 Hz: 19.3 ± 1.2 pg XG equiv. cell $^{-1}$; 1 Hz: 19.3 ± 2.2 pg XG equiv. cell $^{-1}$) (Figure 14 and Table 2).

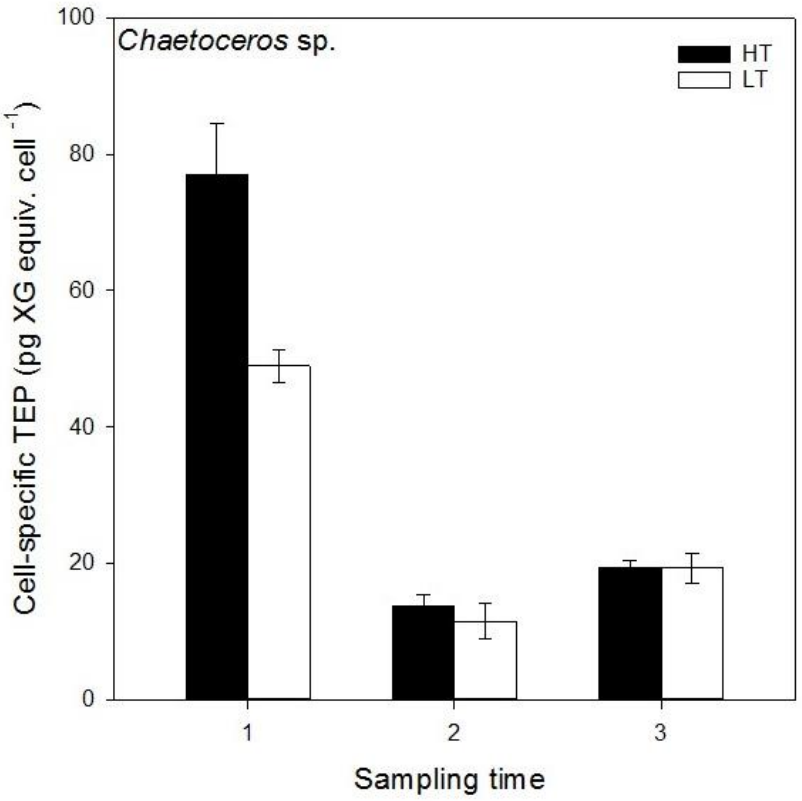

Figure 14 | Cell-specific TEP for the *Chaetoceros* sp. monoculture incubation. HT (solid bars) stands for high turbulent tanks and LT (white bars) stands for low turbulent tanks. Numbers on the x-axis indicate the sampling time point. Error bars are analytical replicates at each sampling time point.

Thalassiosira pseudonana

Volumetric TEP increased throughout the experiment for all three tanks (Table 2). Initial TEP values were 110 ± 34 µg XG equiv. L^{-1} (2 Hz), 140 ± 47 µg XG equiv. L^{-1} (1 Hz), and 139 ± 48 µg XG equiv. L^{-1} (0.5 Hz) (Table 2). From the first to second sampling, TEP concentrations remained relatively constant; between the second and the third time point, TEP increased by a factor of about 4 (2 Hz), 3 (1 Hz), and 2 (0.5 Hz) from the first to third sampling time point (Table 2). In all three tanks, highest volumetric TEP concentrations were measured at the fourth and final sampling time point (2 Hz: 611 ± 165 µg XG equiv. L^{-1}; 1 Hz: 835 ± 143 µg XG equiv. L^{-1}; 0.5 Hz: 636 ± 90 µg XG equiv. L^{-1}) (Table 2).

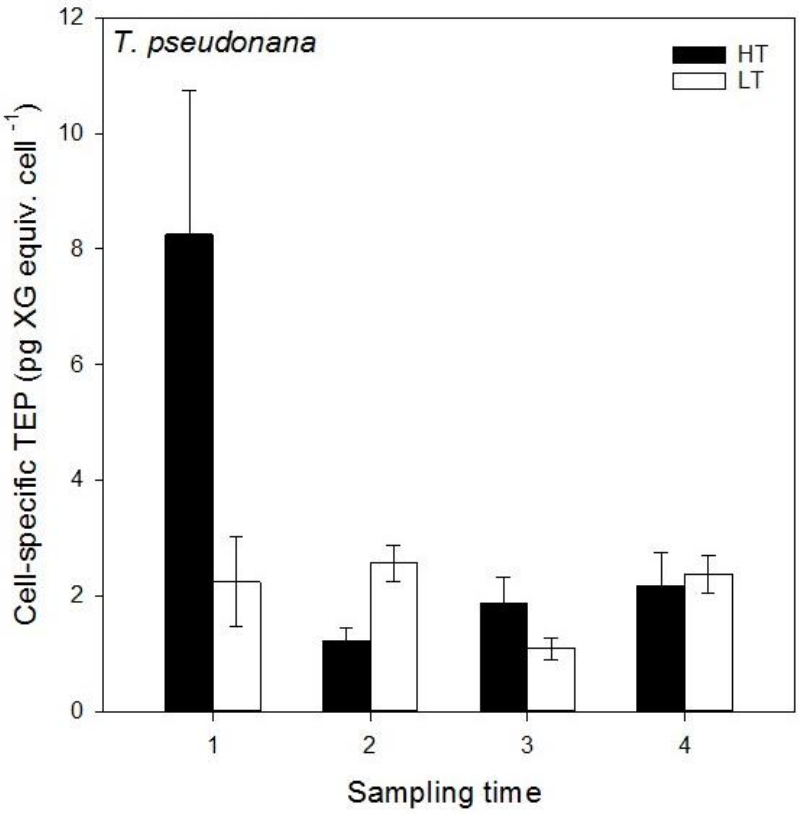

Figure 15 | Cell-specific TEP for the *T. pseudonana* monoculture incubation. HT (solid bars) stands for high turbulent tanks and LT (white bars) stands for low turbulent tanks. Numbers on the x-axis indicate the sampling time point. Error bars are analytical replicates at each sampling time point.

For the high and medium mixing tanks, highest cell-specific TEP values were found at the first time point (2 Hz: 8.25 ± 2.5 pg XG equiv. cell $^{-1}$; 1 Hz: 15.8 ± 5.3 pg XG equiv. cell $^{-1}$) (Figure 15 and Table 2). TEP per cell decreased from the first to second sampling by a factor of about 7 and 9.5 in the 2 Hz and 1 Hz mixing tanks, respectively (Figure 15 and Table 2). Lowest cell-specific TEP concentrations were found in the 0.5 Hz mixing tank at the first sampling (2.24 ± 0.78 pg XG equiv. cell $^{-1}$); TEP per cell at 0.5 Hz remained low throughout the incubation, ranging between 1.09 ± 0.19 pg XG equiv. cell $^{-1}$ and 2.86 ± 0.56 pg XG equiv. cell $^{-1}$ (Figure 15 and Table 2).

Phaeocystis globosa

Initial volumetric TEP concentrations were similar in the three tanks, ranging between 258 ± 12 µg XG equiv. L^{-1} (0.5 Hz) and 317 ± 41 µg XG equiv. L^{-1} (2 Hz) (Table 2). For all three tanks, volumetric TEP concentrations stayed relatively constant from the first to second sampling time point (2 Hz: 309 ± 10 µg XG equiv. L^{-1}; 1 Hz: 269 ± 26 µg XG equiv. L^{-1}; 0.5 Hz: 258 ± 12 µg XG equiv. L^{-1}). From the second to the third time point, volumetric TEP concentrations

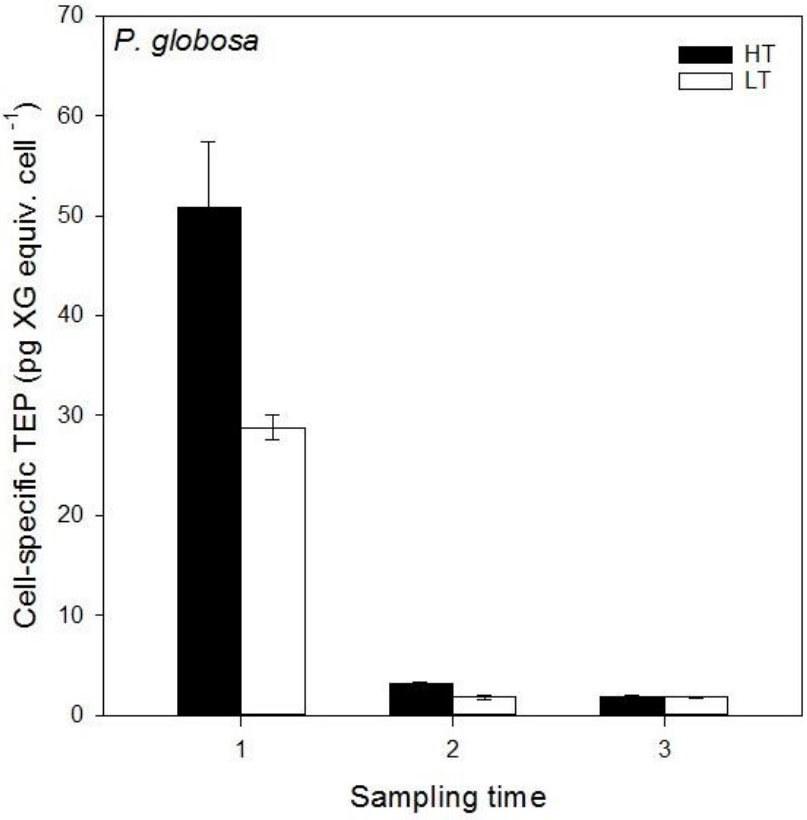

Figure 16 | Cell-specific TEP for the *P. globosa* monoculture incubation. HT (solid bars) stands for high turbulent tanks and LT (white bars) stands for low turbulent tanks. Numbers on the x-axis indicate the sampling time point. Error bars are analytical replicates at each sampling time point.

increased by a factor of about 1.5 in the high and low mixing tanks, and decreased by a factor of about 1.3 in the 1 Hz mixing tank (Table 2).

Highest TEP concentrations per cell in all three tanks were measured at the first time point (Figure 16 and Table 2). Cell-specific TEP was about 2 times higher in the highest turbulent mixing tank (50.8 ± 6.6 pg XG equiv. cell $^{-1}$) than in the 1 Hz (21.1 ± 1.7 pg XG equiv. cell $^{-1}$) and 0.5 Hz (28.8 ± 1.3 pg XG equiv. cell $^{-1}$) tanks. From the first to second time point, cell-specific TEP decreased by about 90% in all three tanks. Cell-specific TEP values were the lowest at the third and final sampling, ranging from 0.9 ± 0.1 pg XG equiv. cell $^{-1}$ to 1.9 ± 0.1 pg XG equiv. cell $^{-1}$ in all three tanks (Figure 16 and Table 2).

Offshore natural assemblages

For the offshore experiment, lowest volumetric TEP values were found at T0 (255 ± 38 µg XG equiv. L^{-1}) (Table 4). In both high and low mixing tanks, volumetric TEP remained constant during the first 48 hours of the incubations. TEP in the high mixing tank gradually increased after T48, reaching highest values at T90 (425 ± 160 µg XG equiv. L^{-1}). In the low mixing tank, highest TEP values were measured at T66 (457 ± 53 µg XG equiv. L^{-1}), following a decrease of TEP until the end of the incubation (Table 4).

TEP per unit chlorophyll in the bulk water (T0) was 2-3 times higher (564 ± 85 µg XG equiv. µg Chl $^{-1}$) than during the incubation (Figure 17 and Table 4). For the high and low mixing tanks, lowest chlorophyll-specific TEP concentrations were measured at T48 (2 Hz: 177 ± 19 µg XG equiv. µg Chl $^{-1}$; 1 Hz: 182 ± 13 µg XG equiv. µg Chl $^{-1}$) (Figure 17 and Table 4). TEP per unit chlorophyll increased slightly (by a factor of 1.3 in the 2 Hz mixing tank and 1.6 in the 1 Hz mixing tank) from T48 to T66. For the last 24 hours of the experiment, TEP per unit chlorophyll stayed somewhat constant, ranging between 262 ± 97 µg XG equiv. µg Chl $^{-1}$ and 219 ± 101 µg XG equiv. µg Chl $^{-1}$ in the high and low mixing tanks (Figure 17 and Table 4).

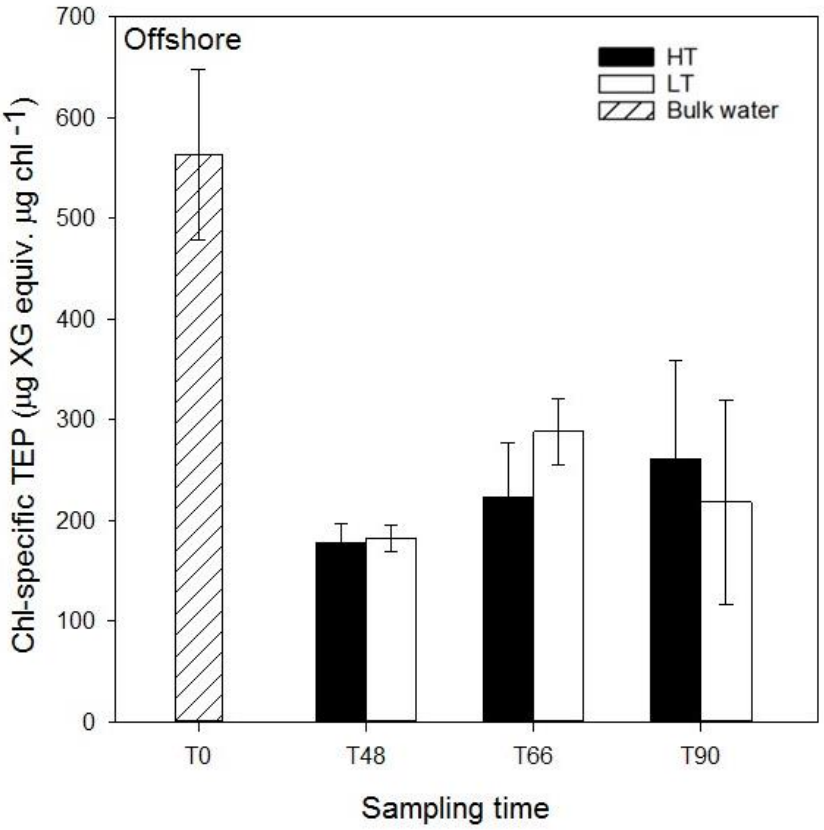

Figure 17 | Chl-specific TEP for the offshore incubation. Note: data collected at T0 (striped bar) was from bulk incubation water. HT (solid bars) stands for high turbulent tanks and LT (white bars) stands for low turbulent tanks. T0, T24, T48, T66, and T90 on the x-axis indicate the sampling time (hours). Error bars are analytical replicates at each sampling time point.

Estuarine natural assemblages

Initial volumetric TEP concentrations were 162 ± 59 µg XG equiv. L^{-1} (Table 4). During the first 24 hours of the experiment, TEP increased by a factor of about 2 in the high mixing tank; at the same time, TEP showed only minor changes in the 1 and 0.5 Hz tanks. In the 2 Hz tank, highest volumetric TEP concentrations were found at T48 (485 ± 49 µg XG equiv. L^{-1}), followed by a 40% decrease until T72 (Table 4). For the medium and low mixing tanks, highest volumetric TEP concentrations were found at T72 (1 Hz: 222 ± 45 µg XG equiv. L^{-1}; 0.5 Hz: 218 ± 61 µg XG equiv. L^{-1}).

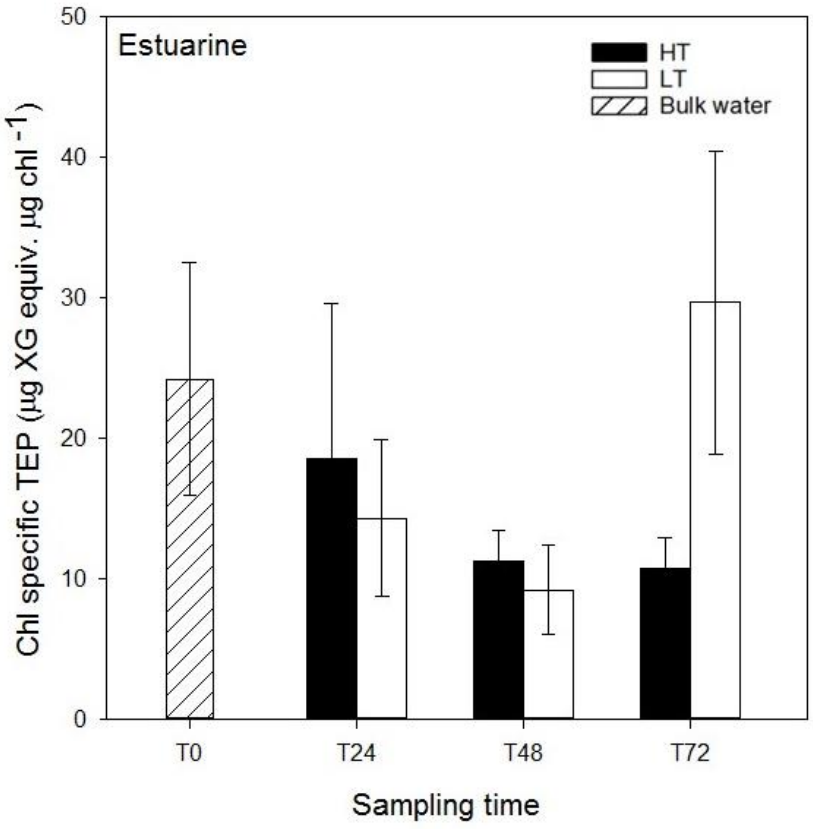

Figure 18 | Chl-specific TEP for the estuarine incubation. Note: data collected at T0 (striped bar) was from bulk incubation water. HT (solid bars) stands for high turbulent tanks and LT (white bars) stands for low turbulent tanks. T0, T24, T48, and T72 on the x-axis indicate the sampling time (hours). Error bars are analytical replicates at each sampling time point.

Chlorophyll-specific TEP in the bulk water (T0) was 24 ± 8 µg XG equiv. µg Chl $^{-1}$ (Figure 18 and Table 4). Values decreased in the first 24 hours by about 20%, 70%, and 40% for the 2, 1, and 0.5 Hz mixing tanks, respectively. In the high mixing tank, chlorophyll-specific TEP values remained constant between T48 (11 ± 2 µg XG equiv. µg Chl $^{-1}$) and T72 (11 ± 2 µg XG equiv. µg Chl $^{-1}$) (Figure 18 and Table 4). In the medium and low mixing tank, chlorophyll-specific TEP increased by a factor of about 3.2 and 2.4, respectively, between T48 and T72, reaching 30 ± 11 µg XG equiv. µg Chl $^{-1}$ (0.5 Hz) and 16 ± 3 µg XG equiv. µg Chl $^{-1}$ (1 Hz) (Figure 18 and Table 4).

5. Discussion

This study used four different phytoplankton of varying sizes and ecological niches in monoculture and obtained natural assemblages from the North Atlantic and Great Bay Estuary. The cells were subjected to a range of turbulent conditions with dissipation rates ranging from 0.02 cm^2 s^{-3} to 1.2 cm^2 s^{-3}. The lowest dissipation rate, 0.02 cm^2 s^{-3}, is similar to observed values in the open ocean, where water mixing is driven by wind (Kahl et al., 2008). Water mixing conditions associated with the middle two dissipation rates, 0.52 cm^2 s^{-3} and 1.2 cm^2 s^{-3}, are similar to a high turbulent system such as an estuary with tidal mixing (Kahl et al., 2008; Petersen et al., 1998) or in the surface waters in the Gulf of Maine during a typical winter storm with wind speeds ~20 m s^{-1} (wind speeds were approximated from MacKenzie and Leggett (1993)). The highest dissipation rate used in this study, 1.2 cm^2 s^{-3}, likely does not reflect mixing ranges found in a steady state marine environment but could be measured during a storm event (ie., a hurricane) with wind speeds exceeding 40 m s^{-1} (Alldredge et al., 1990; Guadayol et al., 2009; Kahl et al., 2008; MacKenzie and Leggett, 1993). Additionally, turbulence levels of this intensity might be seen in future oceans that experience increases in wind-driven surface mixing due to global climate change (Fan et al., 2013; Hemer et al., 2013a, 2013b).

5.1 Effects of turbulence on phytoplankton growth

Growth rate results from the monocultures experiments indicate that the effects of increase turbulence on phytoplankton growth were not measurable (Table 1). These results do not agree with the first part of my hypothesis and also conflict with results from recent studies that found increased phytoplankton growth in higher turbulent experiments (Beauvais et al., 2006; Hondzo and Wüest, 2009; Iversen et al., 2010; Peters et al., 2006). In one study,

Coscinodiscus sp. (cell length ~100 µm) growth rate was 0.37 ± 0.052 day^{-1} in a still tank and 0.42 ± 0.008 day^{-1} in a high turbulent tank (Peters et al., 2006). Additionally, Hondzo and Wuest (2009) found that *E. coli* (cell length ~3 µm) grew 5 times better in the high turbulent treatments when compared to a still tank. One possible explanation for the conflicting results between this study and previous literature could be explained by sedimentation. The previous studies compared growth of phytoplankton in still tanks (with no added turbulence) to growth in high mixing tanks (ε ranging from 1 x 10^{-5} cm^2 s^{-3} to 10 cm^2 s^{-3}). Sedimentation of phytoplankton at the bottom of the tank was recorded in all of the studies that used a still tank as their low turbulent environment (Beauvais et al., 2006; Hondzo and Wüest, 2009; Iversen et al., 2010; Peters et al., 2006). In this study, for the monocultures and offshore experiment, the lower limit of mixing frequency for each monoculture was determined by the lowest amount of introduced turbulence that kept the cells in suspension. Sedimentation was not a factor in the tanks in these experiments and the lowest ε in the incubations with the larger cells (*Thalassiosira* sp., *Chaetoceros* sp., and offshore) was 0.16 cm^2 s^{-3} and the lowest dissipation rate was 0.02 cm^2 s^{-3} in incubations with the smaller cells (*T. pseudonana* and *P. globosa)*. The estuarine incubation was the only experiment where settling out was not controlled and sedimentation was recorded in the low and medium mixing tanks at T24, with the most settling out recorded in the lowest mixing tank. Similarly, at T48 there was settling out in all three tanks and the largest amount of sedimentation was in the lowest mixing tank and the lowest sedimentation was in the highest mixing tank (confirmed with visual observations). A sample of the particles that settled out in all three tanks was examined under the microscope and it was a mixture of phytoplankton and organic matter. Growth rate results from the estuarine incubation agree with previous studies and showed that increased turbulence enhances phytoplankton growth (Beauvais et al., 2006; Hondzo

and Wüest, 2009; Iversen et al., 2010; Peters et al., 2006) (Table 3). This was the only incubation in this study where there was sedimentation and the growth rate is ~2 times higher in the 2 Hz mixing tank than in the 0.5 Hz mixing tank. Results from this study might suggest that increased growth in phytoplankton incubations could have more to do with the amount of sedimentation in the tanks rather than the direct effect of increased turbulence. The effects of turbulence on sedimentation are not well understood because according to fluid dynamic theory and plankton models, there should be enough turbulence (driven solely by density differences in the water) in a still cylindrical tank to keep phytoplankton cells of this size range in suspension (Kiørboe and Hansen, 1993; Peters et al., 2006; Ross, 2006). Yet in the test incubations done for this study and according to previous literature, sedimentation is observed at much higher dissipation rates than predicted by numerical models (Beauvais et al., 2006; Hondzo and Wüest, 2009; Iversen et al., 2010; Peters et al., 2006). It is important to minimize settling out of cells in the tanks when studying the effects of small-scale turbulence on planktonic organisms because when a cell settles out it sits on the bottom of the tank. The nutrient concentration boundary layer, the key parameter that changes based on the amount of turbulence in each tank, becomes reduced in size because half of the boundary layer is blocked by the bottom of the tank. If cells are at the bottom of the tank in the lower mixing treatments, the effects of turbulence on the nutrient concentration boundary layer will be minimized, potentially skewing the results from the study.

To further investigate the small changes in growth rates in the turbulent treatments, the variability in growth rates from the maintenance cultures was examined. While being maintained, the cultures were transferred during mid-exponential growth and growth rates were calculated using the same process as for the larger incubations (see *3.4.2*). Maintenance cultures were kept on a roller table to ensure the cells stayed in suspension. The variability in growth

rates, as defined by percent error, from week to week in the maintenance cultures (*Thalassiosira* sp.: 20%; *Chaetoceros* sp.: 15%; *T. pseudonana*: 15%; *P. globosa*: 17%) was similar to the percent error in the tank incubations with varying turbulence (*Thalassiosira* sp.: 25%; *Chaetoceros* sp.: 20%; *T. pseudonana*: 2%; *P. globosa*: 3%). The range of growth rates found in the varying turbulent treatments reflects the standard amount of variation between growth rates in monoculture. Percent error in the turbulent tanks mentioned above also includes growth rates obtained from replicated *Thalassiosira* sp. and *Chaetoceros* sp. experiments (see *3.2*).

This study also used active fluorescence to further investigate the photophysiological status of the phytoplankton in the varying turbulence tanks. Some ecological stressors (like low nutrient availability and light intensity) causes F_v/F_m to decrease, as well as growth rates (Geider et al., 1993a, 1993b). In this study, F_v/F_m values for these experiments did not differ among the increasing turbulent conditions, suggesting that the photosynthetic efficiency was not altered by the different turbulent conditions (Table 1). Additionally, the small differences in growth rates (Table 1) from this study and previous studies that cultured phytoplankton under increased turbulence (Peters et al., 2006) do not compare with large differences in growth rates (~50%) that are measured when cells are stressed by limiting nutrients, light, or changing other environmental parameters (Cohen et al., 2017; Ellis et al., 2017). In one study, the growth rate of iron-limited pennate diatoms was 0.6 day^{-1}, a 60% reduction when compared to the iron-replete treatment (1.7 day^{-1}) (Cohen et al., 2017). From the same study, F_v/F_m measurements were 0.6 in the stressed low-iron treatment as compared to 0.7 in the high iron incubations. Each species of phytoplankton has a specific maximum growth rate that can be achieved if the environmental conditions are right (Guillard, 1973). When cells are stressed because nutrient concentrations are low or there is too much or too little light for that specific type of phytoplankton, growth rates

are lower than the maximum growth rate for that species (Brand et al., 1981; Eilers and Peeters, 1988; Guillard, 1973). In this study, maximum growth rates for each monoculture were reached in all of the turbulent treatments, meaning that the changes in turbulence in the different treatments were not by itself changing the physical environment around the phytoplankton and inducing stress on the phytoplankton community. Based on the small changes in growth rates from this study and taking into account the data from other studies that found growth rate reductions of ~50% in stress-inducing treatments, perhaps the small increases in phytoplankton growth rates under increased turbulence from previous studies (Iversen et al., 2010; Peters et al., 2006) should not be considered a strong indicator of a positive relationship between phytoplankton growth and increasing turbulence.

Another metric we considered when examining the growth conditions were cellular nutrient quotas. Results from these calculations suggest that in the *Thalassiosira* sp., *Chaetoceros* sp., and offshore experiment, more nutrients were utilized per cell during exponential growth in the higher mixing tanks (Figure 7, Table 1, and Table 3). This result is surprising because in the *Thalassiosira* sp. and *Chaetoceros* sp. incubations, the difference in nutrient quotas was not reflected in the growth rates or TEP production for the higher mixing tanks (Table 1). Additionally, in the offshore experiment, the growth rate for the 1 Hz mixing tank was 1.2 times higher than that of the 2 Hz mixing tank but the N quota was still higher for the cells in the 2 Hz mixing tank (Table 3). The nutrient quotas were similar in both tanks in the smaller two phytoplankton (*T. pseudonana* and *P. globosa*) incubations (Figure 7 and Table 1). These results could be explained by the range of cell sizes in the experiments. The cells from the offshore experiment were examined under the microscope and most were pennate diatoms around 20 µm in length (results not shown), which is similar to the size range of the

Thalassiosira sp. and *Chaetoceros* sp. cultures used in this experiment. Perhaps as predicted by plankton models and fluid dynamic theory, the larger cells in the higher mixing tanks did experience a disruption of the nutrient concentration boundary layer that lead to more nutrients being incorporated into the cells (Barton et al., 2014; Karp-Boss et al., 1996; Wolf-Gladrow and Riebesell, 1997). Additionally, these types of phytoplankton are known to form chains and could have reached similar lengths as the Kolmogorov length scales in the high mixing tanks and experienced increased diffusion of nutrients towards their cell membrane. This increase in nutrients incorporated into the cells had no effect on the growth rates, indicating (1) the cells in this experiment had enough nutrients to reach their maximum exponential growth rate and (2) the additional nutrients in their cells were not being allocated towards a higher specific growth rate. This increase in nutrient quota is not reflected in the growth or TEP production of the phytoplankton cells indicating that the larger cells were potentially storing the nutrients inside their cells (Pedersen and Borum, 1996).

5.2 Effects of turbulence on TEP dynamics

Volumetric TEP and cell-specific TEP values during stationary phase from the *Chaetoceros* sp. experiment in this study are similar to previously reported values by (Passow, 2002a) for a similar culture (*Chaetoceros affinis*: 1107 µg XG equiv. L^{-1}). However, previously reported stationary phase volumetric TEP values for *Thalassiosira weissflogii* (similar to *Thalassiosira* sp. in this study) and *P. globosa* are about 5 times higher than the volumetric TEP values recorded in this study (Mari et al., 2005; Passow, 2002a). Additionally, cell-specific TEP values from stationary phase during the *Thalassiosira* sp. incubation in this study are about 6 times higher than previously recorded values for a similar culture (Passow, 2002b). It is

important to note that phytoplankton are not the only producers of TEP and TEP-precursors in marine systems and it is likely that heterotrophic bacteria in the monocultures and other organisms in the natural assemblages were also adding organic exudates to the water (Passow, 2002b). Additionally, bacteria can serve as a source or sink of DOM in aquatic ecosystems, as they are both producers and consumers of organic exudates (Guillemette and del Giorgio, 2012; Hoppe, 1991). Therefore, cell and chlorophyll-specific TEP values in this study were used as a comparative tool to rule out the fact that changes in volumetric TEP were solely attributable to changes in the number of phytoplankton in the tanks.

In the monocultures, cell-specific and volumetric TEP values from the second and third sampling time points were not substantially different among the different turbulence treatments (Table 2). These results suggest that for the range of turbulences tested and the specific phytoplankton types cultured, the effects of turbulence on phytoplankton TEP production were not substantial. For the *Thalassiosira* sp. and *Chaetoceros* sp. experiments (the larger of the four phytoplankton), there was a 99% drawdown of N from the first to second sampling, indicating that the cells were likely nutrient limited by the second water sampling. If phytoplankton metabolism was affected greatly by the increases in turbulence, we would expect to see different cell-specific and volumetric TEP values in the higher turbulent treatments at the second sampling time point. However, the results from this study indicate that the increased turbulence in the tanks did not have a measurable effect on TEP production during the nutrient-limited sampling times. In the *T. pseudonana* and *P. globosa* experiments, there was a wider range of DIN draw down from the first to second sampling (50 – 90%), so the cells were not fully nutrient limited until the third sampling but again, there is not a substantial difference in the cell-specific TEP in

the higher turbulence tanks for either the second or third sampling time point (Figures 13 – 16 and Table 2).

TEP data from the incubation done with the offshore natural assemblage exhibits similar patterns (Figures 17 and Table 4). There is not a measurable difference in the volumetric TEP or chlorophyll-specific TEP in the higher mixing tanks for the offshore experiment (Table 4). Interestingly, TEP results from the estuarine experiment suggest that there was a positive relationship between increased turbulence and volumetric TEP. Since there is no substantial difference in the chlorophyll-specific TEP between the high and low mixing tanks (Figure 18), it is likely that the increased volumetric TEP in the higher mixing tank is because there were simply more phytoplankton in the higher mixing tank.

In all four monoculture experiments, there was substantially higher cell-specific TEP values at the first sampling time point (Figures 13 – 16). The results are somewhat surprising because from inoculation to the first water sampling, DIN is replete in the tanks (Table 2). Based on fluid dynamics theory and previous model investigations, I expected to see a difference in TEP production when nutrients were decreasing because the nutrient concentration boundary layer becomes an important factor determining the amount of nutrients that surrounding the cell (Barton et al., 2014; Karp-Boss et al., 1996).

Growth rates are similar in the treatments and the higher cell-specific TEP values were found only during the first sampling time point when nutrients were replete so it is likely that the increased cell-specific TEP values in the higher turbulent tanks are not due to a metabolic change in the phytoplankton cells. Taking this assumption into consideration, a physical parameter might be responsible for these higher cell specific values at the first sampling time point. Models and experiments have shown that turbulence increases particle encounter rates during marine snow

aggregate formation (Brunk et al., 1998; Hill et al., 1992; Jackson, 1990; Kiørboe, 1997). DOM produced by marine organisms can range in size from colloidal to particulate matter and the phrase "particles" in this study refers to anything large enough to stick on the 0.4 µm polycarbonate filters. Organic exudates that go on to form TEP are surface reactive and if they encounter each other more frequently in the higher mixing tanks, that could lead to an increased number of larger, sticky TEP particles. The method used (see *3.4.5*) is semi-quantitative and useful for comparing TEP concentrations between treatments but does not give information on the size of the TEP. The preserved TEP slides with filters were examined using light microscopy to investigate if there was a noticeable increase in size of TEP particles in the higher turbulence tanks. A size differential in TEP particles among the varying turbulent treatments at the first sampling time was not detectable because TEP on the filters was mostly associated with the phytoplankton cells making it difficult to decipher changes in TEP size (Figure 19).

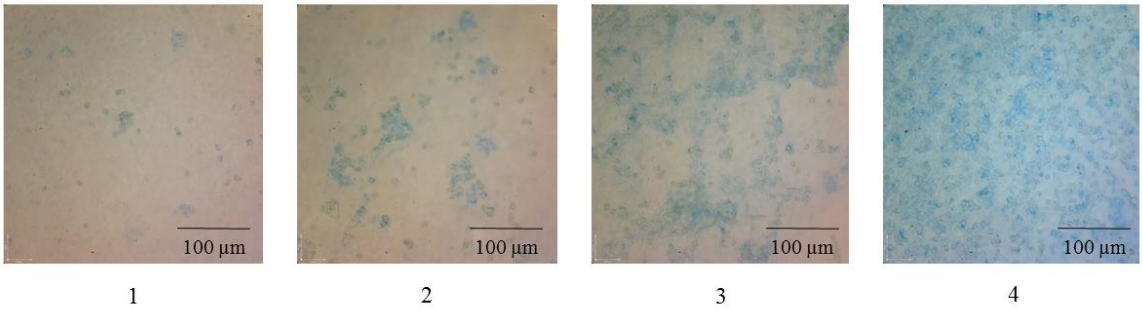

Figure 19 | TEP filters from *T. pseudon*ana experiment. The blue on each filter are TEP acidic polysaccharides stained with Alcian Blue (see analytical methods for more details). Numbers 1 – 4 indicate the sampling time point when the water samples were taken and filters made.

Higher cell-specific TEP in the higher turbulent treatments is not seen in the later sampling time points for the monocultures and incubations with the natural assemblages. One explanation is that perhaps the physical aspect of encounter rates was diminished because of the role heterotrophic bacteria were playing in transforming and degrading the TEP matrices. For the

monocultures, volumetric TEP concentrations were low at the first sampling time point in all three of the monoculture experiments so the TEP pool was small, phytoplankton and bacterial counts were low, and bacteria might have been breaking down TEP at a low rate (Table 2). During the later sampling time points, volumetric TEP increased and encounter rates were still higher in the higher turbulent tanks, but perhaps the heterotrophic bacteria in all three mixing tanks were acting more as a sink, by transforming and degrading TEP. In the natural assemblages, there were multiple different types of phytoplankton and bacteria, ambient sources of DOM and likely other aquatic organisms in the water at the time of sampling that made the TEP production and utilization dynamics more complicated from the start. These complex phytoplankton-bacteria-TEP interactions could have diminished the physical effect of increased encounter rates during the later sampling time points in the monocultures and throughout the incubations with the natural assemblages, explaining why the higher encounter rates in the higher turbulent tanks did not lead to higher cell-specific TEP. Along the same lines, it is possible that there was a metabolic effect of turbulence on TEP production in the incubations but that the changes were not measurable because of the complicated role that heterotrophic bacteria play as a sink of phytoplankton-derived organic exudates.

To further investigate the role that bacteria were playing in diminishing the effects of turbulence on TEP production, (1) the concentration of TEP-carbon (TEP-C) that was "missing" from the cell-specific TEP values in the high mixing tank at the third sampling time point, (2) the concentration of C that went into bacterial biomass production in the high mixing tank, and (3) concentration of C that went into bacterial biomass production in the low mixing tank were calculated for all four monoculture experiments. These numbers were used to investigate if the

fraction of TEP-C that was being degraded and transformed in the later sampling time point could realistically be going towards the bacterial biomass increases measured in the tanks.

First, the percent increase due to increased encounter rates in the high mixing tank was calculated by comparing the cell-specific TEP values in the high and low mixing tank at the first sampling time point. Using the percent increase for each individual monoculture and assuming the percent increase due to turbulence did not change from the first to third sampling time point, a theoretical cell-specific TEP concentration was calculated for the high mixing tank at the third sampling time point. Next, the difference in the theoretical and measured cell-specific TEP concentration at the third sampling time point was calculated and assumed to be the "missing" TEP due to bacterial degradation. To calculate TEP-C in that missing fraction, it was assumed that in 1 µg XG equiv. there are ~0.75 µg C (Engel and Passow, 2001). Next, to calculate the concentration of C that went into bacterial biomass production, the increase in bacteria cells from the first to third sampling time point was multiplied by the average concentration of C in bacterial cells associated with phytoplankton during bloom cycles (~30 fg C per bacterial cell, adapted from Fukuda et al. (1998)). Note that in two instances (*Thalassiosira* sp. 2 Hz tank and *P. globosa* 0.5 Hz tank) bacterial biomass peaked the day right before the third sampling so the higher bacteria cell concentration was used for these calculations. Using the maximum bacterial cell concentration gives a more realistic estimate for the amount of carbon utilized by the bacteria for biomass.

The results from these calculations indicate that the missing C in the high mixing tank at the final sampling time point is comparable to the increase in bacterial biomass in both the high and low mixing tanks (Figure 20). The amount of C going into bacterial biomass production is lower or comparable in the high mixing tank compared to the low mixing tank in all but the *P.*

globosa incubation. These calculations do not confirm or disprove that bacteria degradation and transformation of the TEP is directly responsible for the missing higher cell-specific TEP concentration in the high mixing tank at the later sampling time points. Rather, they show that the order of magnitude for the missing TEP-C is similar to the amount of C that went into

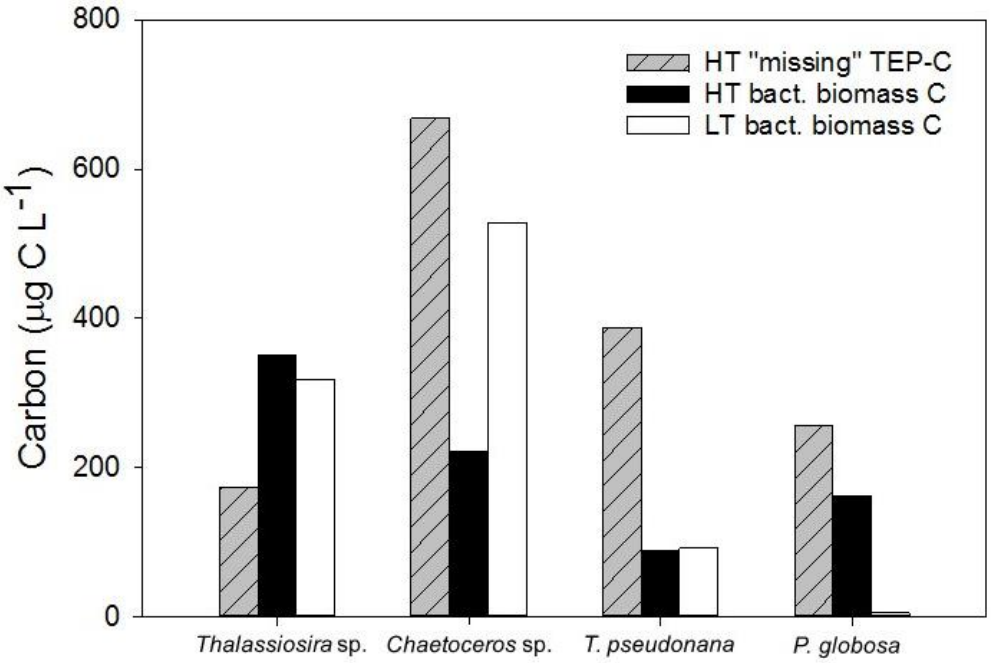

Figure 20 | Carbon loss estimates for the monoculture incubations. Concentration of TEP-carbon "missing" in the high turbulent (HT, gray striped bars), concentration of TEP-carbon loss attributable to bacterial biomass in the high turbulent (HT, black bars) tanks, and concentration of TEP-carbon loss attributable to bacterial biomass in the low turbulent (LT, white bars) tanks.

bacterial biomass production. It is possible that the bacteria were in fact transforming and degrading the TEP in the higher mixing tanks, diminishing the effects of turbulence on the measured cell-specific concentrations, but they just were not using the C for biomass production. Bacteria also contribute to the DOM pool so it is possible that the bacteria in the high mixing tanks were responsible for diminishing the effects of turbulence on cell-specific TEP, but that instead of that C being put towards making more bacteria cells, it was released in to the water in

the form of DOM too small to show up on the 0.4 µm filters used to quantify TEP concentrations.pdersen

5.3 Implications for the marine carbon cycle in a more turbulent ocean

Our current understanding of the effects of small-scale turbulence on marine phytoplankton growth and metabolism is poorly constrained. Investigating how TEP production is affected by changes in small-scale turbulence is an important link in understanding how the global carbon cycle will be affected by global climate change. The results from this study suggest that while there may be increased nutrient fluxes for larger phytoplankton cells (>15 µm in length) in higher turbulent environments, the effects on phytoplankton growth and TEP production are not substantial. However, the implications of changes in nutrient cell quotas might influence other phytoplankton cellular processes, such as nutrient storage, in large phytoplankton cells in high turbulent marine ecosystems. Increased nutrient storage by large phytoplankton cells could have substantial effects on phytoplankton bloom duration and community composition, affecting the role they play in the global carbon and oxygen cycles and in their role as the base of the marine food web. Traditionally, small phytoplankton out-compete large phytoplankton in low nutrient aquatic ecosystems because of their increased surface area to volume ratio (Agusti et al., 1987; Sheldon et al., 1972). However, based on the results from this study, it is possible that in a marine ecosystem with high turbulent kinetic energy but low nutrient concentrations, large phytoplankton could have a competitive advantage, via enhanced nutrient storage, over small phytoplankton cells that are not experiencing the increased nutrient flux caused by turbulence.

6. Conclusions

The goals of this study were to better understand how small-scale turbulence affects phytoplankton growth and metabolism by examining culture growth rates, nutrient quotas, heterotrophic bacterial biomass, and TEP production. This study differs from previous studies investigating the effects of turbulence on phytoplankton growth because the effects of sedimentation were minimized. The growth rate results do not agree with previous literature and it is possible that sedimentation has a bigger effect than previously realized when culturing phytoplankton in different turbulent environments.

I recommend future studies that focus on the effects of small-scale turbulence during the beginning stages of phytoplankton growth. The higher cell-specific TEP results found at the first sampling time point in these incubations are interesting and should be explored further. Currently most studies look at TEP production in the stationary phase because TEP production increases when the cells are nutrient limited, however, results from this study suggest that physical processes could be affecting the TEP concentrations at the beginning of the growth cycle when nutrients are replete and the cells are exponentially growing. I also recommend further experiments in which the cultures are carried out axenically. Not having the bacteria present would help better understand phytoplankton-bacterial interactions and the role heterotrophic bacteria play in TEP production and utilization. Additionally, studies in which chemostats are used would create a nutrient-limited environment that is more analogous to that of a typical open ocean ecosystem. Batch cultures, the culturing method used in this study, have a very short time period in which a nutrient concentration boundary layer could develop but chemostats set a fixed growth rate by introducing a constant, low concentration of nutrients to the phytoplankton cells.

Examining the nutrient quotas during a chemostat experiment would better target the effects of small-scale turbulence on the potential disruption of a nutrient concentration boundary layer.

7. References

Agusti, S., Duarte, C. M., and Kalff, J. (1987). Algal cell size and the maximum density and biomass of phytoplankton1. *Limnol. Oceanogr.* 32, 983–986. doi:10.4319/lo.1987.32.4.0983.

Alldredge, A. L., Granata, T. C., Gotschalk, C. C., and Dickey, T. D. (1990). The physical strength of marine snow and its implications for particle disaggregation in the ocean. *Limnol. Oceanogr.* 35. Available at: http://m.m.aslo.info/lo/toc/vol_35/issue_7/1415.pdf [Accessed March 3, 2017].

Alldredge, A. L., and Silver, M. W. (1988). Characteristics, dynamics and significance of marine snow. *Prog. Oceanogr.* 20, 41–82. doi:10.1016/0079-6611(88)90053-5.

Arin, L., Marras, C., Maar, M., Peters, F., Sala, M., and Alcaraz, M. (2002). Combined effects of nutrients and small-scale turbulence in a microcosm experiment. I. Dynamics and size distribution of osmotrophic plankton. *Aquat. Microb. Ecol.* 29, 51–61. doi:10.3354/ame029051.

Armstrong, R. A., Lee, C., Hedges, J. I., Honjo, S., and Wakeham, S. G. (2001). A new, mechanistic model for organic carbon fluxes in the ocean based on the quantitative association of POC with ballast minerals. *Deep Sea Res. Part II Top. Stud. Oceanogr.* 49, 219–236. doi:10.1016/S0967-0645(01)00101-1.

Barton, A. D., Ward, B. A., Williams, R. G., and Follows, M. J. (2014). The impact of fine-scale turbulence on phytoplankton community structure. *Limnol. Oceanogr. Fluids Environ.* 4, 34–49. doi:10.1215/21573689-2651533.

Beauvais, S., Pedrotti, M. L., Egge, J., Iversen, K., and Marras, C. (2006). Effects of turbulence on TEP dynamics under contrasting nutrient conditions: implications for aggregation and sedimentation processes. *Mar. Ecol. Prog. Ser.* 323, 47–57. doi:10.3354/meps323047.

Brand, L. E., Guillard, R. R. L., and Murphy, L. S. (1981). A method for the rapid and precise determination of acclimated phytoplankton reproduction rates. *J. Plankton Res.* 3, 193–201. doi:10.1093/plankt/3.2.193.

Brunk, B. K., Koch, D. L., and Lion, L. W. (1998). Observations of coagulation in isotropic turbulence. *J. Fluid Mech.* 371, 81–107.

Cohen, N. R., A Ellis, K., Burns, W. G., Lampe, R. H., Schuback, N., Johnson, Z., et al. (2017). Iron and vitamin interactions in marine diatom isolates and natural assemblages of the Northeast Pacific Ocean. *Limnol. Oceanogr.* Available at: http://onlinelibrary.wiley.com/doi/10.1002/lno.10552/full [Accessed May 7, 2017].

DeVries, T., Primeau, F., and Deutsch, C. (2012). The sequestration efficiency of the biological pump. *Geophys. Res. Lett.* 39. Available at: http://onlinelibrary.wiley.com/doi/10.1029/2012GL051963/full [Accessed March 3, 2017].

Edwards, M., and Richardson, A. J. (2004). Impact of climate change on marine pelagic phenology and trophic mismatch. *Nature* 430, 881–884. doi:10.1038/nature02808.

Eilers, P. H. C., and Peeters, J. C. H. (1988). A model for the relationship between light intensity and the rate of photosynthesis in phytoplankton. *Ecol. Model.* 42, 199–215. doi:10.1016/0304-3800(88)90057-9.

Ellis, K. A., Cohen, N. R., Moreno, C., and Marchetti, A. (2017). Cobalamin-independent Methionine Synthase Distribution and Influence on Vitamin B12 Growth Requirements in Marine Diatoms. *Protist* 168, 32–47. doi:10.1016/j.protis.2016.10.007.

Engel, A. (2000). The role of transparent exopolymer particles (TEP) in the increase in apparent particle stickiness (α) during the decline of a diatom bloom. *J. Plankton Res.* 22, 485–497. doi:10.1093/plankt/22.3.485.

Engel, A., and Passow, U. (2001). Carbon and nitrogen content of transparent exopolymer particles (TEP) in relation to their Alcian Blue adsorption. *Mar. Ecol. Prog. Ser.* 219, 1–10. doi:Engel, Anja and Passow, U. (2001) Carbon and nitrogen content of transparent exopolymer particles (TEP) in relation to their Alcian Blue adsorption Marine Ecology Progress Series, 219 . pp. 1-10. DOI 10.3354/meps219001 <http://dx.doi.org/10.3354/meps219001>.

EPA (2013). *Methods for the Determination of Metals in Environmental Samples*. Elsevier.

Fan, Y., Isaac Held, Lin, S.-J., and Wang, X. L. (2013). Ocean Warming Effect on Surface Gravity Wave Climate Change for the End of the Twenty-First Century. *J. Clim.* 26, 6046–6066. doi:10.1175/JCLI-D-12-00410.1.

Fukuda, R., Ogawa, H., Nagata, T., and Koike, I. (1998). Direct Determination of Carbon and Nitrogen Contents of Natural Bacterial Assemblages in Marine Environments. *Appl. Environ. Microbiol.* 64, 3352–3358.

Geider, R. J., Greene, R. M., Kolber, Z., MacIntyre, H. L., and Falkowski, P. G. (1993a). Fluorescence assessment of the maximum quantum efficiency of photosynthesis in the western North Atlantic. *Deep Sea Res. Part Oceanogr. Res. Pap.* 40, 1205–1224. doi:10.1016/0967-0637(93)90134-O.

Geider, R. J., La Roche, J., Greene, R. M., and Olaizola, M. (1993b). Response of the Photosynthetic Apparatus of Phaeodactylum Tricornutum (bacillariophyceae) to Nitrate, Phosphate, or Iron Starvation1. *J. Phycol.* 29, 755–766. doi:10.1111/j.0022-3646.1993.00755.x.

Grossart, H.-P., Czub, G., and Simon, M. (2006). Algae–bacteria interactions and their effects on aggregation and organic matter flux in the sea. *Environ. Microbiol.* 8, 1074–1084. doi:10.1111/j.1462-2920.2006.00999.x.

Guadayol, O., Peters, F., Stiansen, J. E., Marrase, C., and Lohrmann, A. (2009). Evaluation of oscillating grids and orbital shakers as means to generate isotropic and homogeneous small-scale turbulence in laboratory enclosures commonly used in plankton studies. *Limnol. Oceanogr. Methods* 7, 287–303.

Guillard, R. R. L. (1973). "Division rates," in *Handbook of Phycological Methods: Culture Methods and Growth Measurements*, 289–312.

Guillemette, F., and del Giorgio, P. A. (2012). Simultaneous consumption and production of fluorescent dissolved organic matter by lake bacterioplankton. *Environ. Microbiol.* 14, 1432–1443. doi:10.1111/j.1462-2920.2012.02728.x.

Hecky, R. E., and Kilham, P. (1988). Nutrient limitation of phytoplankton in freshwater and marine environments: A review of recent evidence on the effects of enrichment1. *Limnol. Oceanogr.* 33, 796–822. doi:10.4319/lo.1988.33.4part2.0796.

Hemer, M. A., Fan, Y., Mori, N., Semedo, A., and Wang, X. L. (2013a). Projected changes in wave climate from a multi-model ensemble. *Nat. Clim. Change* 3, 471–476. doi:10.1038/nclimate1791.

Hemer, M. A., Katzfey, J., and Trenham, C. E. (2013b). Global dynamical projections of surface ocean wave climate for a future high greenhouse gas emission scenario. *Ocean Model.* 70, 221–245. doi:10.1016/j.ocemod.2012.09.008.

Hill, P. S., Nowell, A. R. M., and Jumars, P. A. (1992). Encounter rate by turbulent shear of particles similar in diameter to the Kolmogorov scale. *J. Mar. Res.* 50, 643–668. doi:10.1357/002224092784797539.

Hondzo, M., and Lyn, D. (1999). Quantified small-scale turbulence inhibits the growth of a green alga. *Freshw. Biol.* 41, 51–61. doi:10.1046/j.1365-2427.1999.00389.x.

Hondzo, M., and Wüest, A. (2009). Do Microscopic Organisms Feel Turbulent Flows? *Environ. Sci. Technol.* 43, 764–768. doi:10.1021/es801655p.

Hoppe, H.-G. (1991). "Microbial Extracellular Enzyme Activity: A New Key Parameter in Aquatic Ecology," in *Microbial Enzymes in Aquatic Environments* Brock/Springer Series in Contemporary Bioscience., 60–83. Available at: https://www.researchgate.net/publication/259971841_Microbial_Extracellular_Enzyme_Activity_A_New_Key_Parameter_in_Aquatic_Ecology [Accessed March 25, 2017].

Iversen, K., Primicerio, R., Larsen, A., Egge, J. K., Peters, F., Guadayol, Ó., et al. (2010). Effects of small-scale turbulence on lower trophic levels under different nutrient conditions. *J. Plankton Res.* 32, 197–208. doi:10.1093/plankt/fbp113.

Jackson, G. A. (1990). A model of the formation of marine algal flocs by physical coagulation processes. *Deep Sea Res. Part Oceanogr. Res. Pap.* 37, 1197–1211. doi:10.1016/0198-0149(90)90038-W.

Jumars, P. A. (1993). *Concepts in biological oceanography*. Oxford University Press Available at: http://agris.fao.org/agris-search/search.do?recordID=US201300727435 [Accessed March 24, 2017].

Kahl, L. A., Vardi, A., and Schofield, O. (2008). Effects of phytoplankton physiology on export flux. *Mar. Ecol. Prog. Ser.* 354, 3–19. doi:https://doi.org/10.3354/meps07333.

Karp-Boss, L., Boss, E., Jumars, P. A., and others (1996). Nutrient fluxes to planktonic osmotrophs in the presence of fluid motion. *Oceanogr. Mar. Biol.* 34, 71–108.

Kiørboe, T. (1997). Small-scale turbulence, marine snow formation, and planktivorous feeding. *Sci. Mar.* 61, 141–158.

Kiørboe, T., Andersen, K. P., and Dam, H. G. (1990). Coagulation efficiency and aggregate formation in marine phytoplankton. *Mar. Biol.* 107, 235–245. doi:10.1007/BF01319822.

Kiørboe, T., and Hansen, J. L. (1993). Phytoplankton aggregate formation: observations of patterns and mechanisms of cell sticking and the significance of exopolymeric material. *J. Plankton Res.* 15, 993–1018.

Kiørboe, T., Lundsgaard, C., Olesen, M., and Hansen, J. L. S. (1994). Aggregation and sedimentation processes during a spring phytoplankton bloom: A field experiment to test coagulation theory. *J. Mar. Res.* 52, 297–323. doi:10.1357/0022240943077145.

Koch, A. L. (1971). The Adaptive Responses of Escherichia coli to a Feast and Famine Existence. *Adv. Microb. Physiol.* 6, 147–217. doi:10.1016/S0065-2911(08)60069-7.

Kolmogorov, A. N. (1962). A refinement of previous hypotheses concerning the local structure of turbulence in a viscous incompressible fluid at high Reynolds number. *J. Fluid Mech.* 13, 82–85. doi:10.1017/S0022112062000518.

Long, R. A., and Azam, F. (1996). Abundant protein-containing particles in the sea. *Aquat. Microb. Ecol.* 10, 213.

Lorenzen, C. J. (1967). Determination of Chlorophyll and Pheo-Pigments: Spectrophotometric Equations1. *Limnol. Oceanogr.* 12, 343–346. doi:10.4319/lo.1967.12.2.0343.

MacKenzie, B. R., and Leggett, W. C. (1993). Wind-based models for estimating the dissipation rates of turbulent energy in aquatic environments: empirical comparisons. *Mar. Ecol.-Prog. Ser.* 94, 207–207.

Mari, X., Rassoulzadegan, F., Brussaard, C. P. D., and Wassmann, P. (2005). Dynamics of transparent exopolymeric particles (TEP) production by Phaeocystis globosa under N- or P-limitation: a controlling factor of the retention/export balance. *Harmful Algae* 4, 895–914. doi:10.1016/j.hal.2004.12.014.

Mari, X., and Robert, M. (2008). Metal induced variations of TEP sticking properties in the southwestern lagoon of New Caledonia. *Mar. Chem.* 110, 98–108. doi:10.1016/j.marchem.2008.02.012.

Martin, P., Lampitt, R. S., Jane Perry, M., Sanders, R., Lee, C., and D'Asaro, E. (2011). Export and mesopelagic particle flux during a North Atlantic spring diatom bloom. *Deep Sea Res. Part Oceanogr. Res. Pap.* 58, 338–349. doi:10.1016/j.dsr.2011.01.006.

Monod, J. (1949). The Growth of Bacterial Cultures. *Annu. Rev. Microbiol.* 3, 371–394. doi:10.1146/annurev.mi.03.100149.002103.

Montes-Hugo, M., Doney, S. C., Ducklow, H. W., Fraser, W., Martinson, D., Stammerjohn, S. E., et al. (2009). Recent Changes in Phytoplankton Communities Associated with Rapid Regional Climate Change Along the Western Antarctic Peninsula. *Science* 323, 1470–1473. doi:10.1126/science.1164533.

Passow, and Laws (2015). Ocean acidification as one of multiple stressors: growth response of Thalassiosira weissflogii (diatom) under temperature and light stress. *Mar. Ecol. Prog. Ser.* 541, 75–90.

Passow, U. (2002a). Production of transparent exopolymer particles (TEP) by phyto- and bacterioplankton. *Mar. Ecol. Prog. Ser.* 236, 1–12. doi:10.3354/meps236001.

Passow, U. (2002b). Transparent exopolymer particles (TEP) in aquatic environments. *Prog. Oceanogr.* 55, 287–333. doi:10.1016/S0079-6611(02)00138-6.

Passow, U., and Alldredge, A. L. (1995). A dye-binding assay for the spectrophotometric measurement of transparent exopolymer particles (TEP). *Limnol. Oceanogr.* 40, 1326–1335.

Pedersen, M., and Borum, J. (1996). Nutrient control of algal growth in estuarine waters. Nutrient limitation and the importance of nitrogen requirements and nitrogen storage among phytoplankton and species of macroalgae. *Mar. Ecol. Prog. Ser.* 142, 261–272. doi:10.3354/meps142261.

Peters, F., Arin, L., Marrasé, C., Berdalet, E., and Sala, M. M. (2006). Effects of small-scale turbulence on the growth of two diatoms of different size in a phosphorus-limited medium. *J. Mar. Syst.* 61, 134–148. doi:10.1016/j.jmarsys.2005.11.012.

Petersen, J. E., Sanford, L. P., and Kemp, W. M. (1998). Coastal plankton responses to turbulent mixing in experimental ecosystems. *Mar. Ecol. Prog. Ser.* 171, 23–41. doi:10.3354/meps171023.

Price, N. M., Harrison, G. I., Hering, J. G., Hudson, R. J., Nirel, P. M. V., Palenik, B., et al. (1989). Preparation and Chemistry of the Artificial Algal Culture Medium Aquil. *Biol. Oceanogr.* 6, 443–461. doi:10.1080/01965581.1988.10749544.

Riebesell, U., Reigstad, M., Wassmann, P., Noji, T., and Passow, U. (1995). On the trophic fate of Phaeocystis pouchetii (hariot): VI. Significance of Phaeocystis-derived mucus for vertical flux. *Neth. J. Sea Res.* 33, 193–203. doi:10.1016/0077-7579(95)90006-3.

Ross, O. N. (2006). Particles in motion: How turbulence affects plankton sedimentation from an oceanic mixed layer. *Geophys. Res. Lett.* 33, L10609. doi:10.1029/2006GL026352.

Ruiz, J. (1996). The role of turbulence in the sedimentation loss of pelagic aggregates from the mixed layer. *J. Mar. Res.* 54, 385–406. doi:10.1357/0022240963213367.

Rumyantseva, A., Lucas, N., Rippeth, T., Martin, A., Painter, S. C., Boyd, T. J., et al. (2015). Ocean nutrient pathways associated with the passage of a storm. *Glob. Biogeochem. Cycles* 29, 2015GB005097. doi:10.1002/2015GB005097.

Sheldon, R. W., Prakash, A., and Sutcliffe, W. H. (1972). The Size Distribution of Particles in the Ocean1. *Limnol. Oceanogr.* 17, 327–340. doi:10.4319/lo.1972.17.3.0327.

Siegel, D. A., Buesseler, K. O., Doney, S. C., Sailley, S. F., Behrenfeld, M. J., and Boyd, P. W. (2014). Global assessment of ocean carbon export by combining satellite observations and food-web models. *Glob. Biogeochem. Cycles* 28, 2013GB004743. doi:10.1002/2013GB004743.

Thomas, W. H., and Gibson, C. H. (1990). Effects of small-scale turbulence on microalgae. *J. Appl. Phycol.* 2, 71–77. doi:10.1007/BF02179771.

Toseland, A., Daines, S. J., Clark, J. R., Kirkham, A., Strauss, J., Uhlig, C., et al. (2013). The impact of temperature on marine phytoplankton resource allocation and metabolism. *Nat. Clim. Change* 3, 979–984. doi:10.1038/nclimate1989.

Wolf-Gladrow, D., and Riebesell, U. (1997). Diffusion and reactions in the vicinity of plankton: A refined model for inorganic carbon transport. *Mar. Chem.* 59, 17–34. doi:10.1016/S0304-4203(97)00069-8.